ABSTRACT

Title of Document: **THE EFFECT OF BENTHIC MICROALGAL PHOTOSYSNTHETIC OXYGEN PRODUCTION ON NITROGEN FLUXES ACROSS THE SEDIMENT-WATER INTERFACE IN A SHALLOW, SUB-TROPICAL ESTUARY**

Jessica Landis Burton Evans, Master of Science, 2005

Directed By: Dr. Jeffrey C. Cornwell, Marine, Estuarine and Environmental Science Program

Benthic microalgae (BMA) are a highly productive component of benthic ecosystems. BMA production and nitrogen fluxes were examined in four sub-basins of Florida Bay, in both seagrass and seagrass-free patches, as well as seasonally in a persistent seagrass-free patch in eastern Florida Bay. BMA biomass and oxygen production was highest in seagrass-free sediments with little seasonal variability. Despite high porewater NH_4^+ concentrations there was little NH_4^+ efflux. As in temperate estuaries, sub-tropical BMA production and N-assimilation act as a filter to prevent the release of nutrients to the water column.

Microelectrode measurements revealed that BMA production causes a doubling of the depth to which O_2 penetrates, increasing suitable conditions for nitrification and coupled denitrification. However, the presence of H_2S in surface sediments can inhibit nitrification, and there is little nitrogen removal from Florida Bay by denitrification. As a result, BMA N-assimilation is an important nutrient sink in this oligotrophic estuary.

THE EFFECT OF BENTHIC MICROALGAL PHOTOSYSNTHETIC OXYGEN PRODUCTION ON NITROGEN FLUXES ACROSS THE SEDIMENT-WATER INTERFACE IN A SHALLOW, SUB-TROPICAL ESTUARY

by

Jessica Landis Burton Evans

Thesis submitted to the Faculty of the Graduate School of the
University of Maryland, College Park, in partial fulfillment
of the requirements for the degree of
Master of Science
2005

Advisory Committee:

Dr. Jeffrey C. Cornwell, Chair
Dr. W. Michael Kemp
Dr. Karen J. McGlathery
Dr. William C. Dennison

Acknowledgements

I would like to thank my graduate committee; Drs. Jeff Cornwell, Mike Kemp, Bill Dennison, and Karen McGlathery; for their patience, guidance, support, and understanding. Each, in their own way, has help strengthen my research and me as a researcher. Thanks to all who have supported me through countless hours of field work, lab work, and computer toils, including: Mike Owens, Debbie Hinkle, Jessica Davis, Eric Nagel, Rebecca Holyoke, Erica Kiss, Jennifer O'Keefe, Chris Chick and Sarah Rhoades. Thanks to the UMCES-Horn Point Laboratory Analytical Services Staff for chlorophyll sample processing and use of analytical equipment. I am indebted to the graphical expertise of the Integration and Application Network, Dr. Tim Carruthers, Dr. Adrian Jones, Tracey Saxby and Jane Thomas, for all of their assistance with this thesis and associated presentations. Special thanks to Dr. Carruthers for his assistance with early drafts of this thesis.

Thanks to for the financial support to conduct this research from: Horn Point Laboratory Fellowship and Small Grant Awards, National Science Foundation, and NOAA-SFERPM. Thanks to the Everglades National Park Interagency Science Center, Art Schwarzchild, Tom Frankovich, and the UVA Florida Bay crew for logistical support and advice.

I would like to thank my family and friends, near and far, for supporting me in pursuit of my Masters degree. Finally, I would like to say thank you to my husband,for his emotional support, architectural lighting designs, and assistance in the preparation of thousands of sample vials during the past 3 years. Thank you, Jeff, for all of your love and support.

Table of Contents

List of Tables

List of Figures

Introduction: Benthic microalgae in sub-tropical estuaries

In shallow estuarine and littoral systems worldwide a number of different types of benthic photoautotrophs are important to net ecosystem productivity. Seagrass, macroalgae, and microalgae inhabit the benthos from the high arctic to the tropics, as long as there is sufficient light to support primary production (MacIntyre et al. 1996 and references therein, Glud et al. 2002, Sand-Jensen & Nielsen 2004). All benthic primary producers are important in mediating biogeochemical processes and fluxes at the sediment-water interface. The benthic microalgae (BMA) community, composed of photosynthetic microalgae and cyanobacteria inhabiting surface sediments, is a highly productive component in shallow water ecosystems, especially those that lack macrophytes (MacIntyre et al. 1996). Rates of primary production in BMA communities are comparable to those of macrophytes and phytoplankton (MacIntyre et al. 1996), and as a result, BMA are likely to have important effects on ecosystem-scale nutrient cycling processes (Sand-Jensen & Nielsen 2004). The effects of BMA production on N-cycling are largely known from temperate systems (e.g. Pinckney & Zingmark 1993, Risgaard-Petersen et al. 1994, Sundback & Miles 2000, Dalsgaard 2003). Understanding how benthic primary production affects denitrification and dissolved inorganic nitrogen (DIN) fluxes in sub-tropical and tropical systems is important to develop useful coastal zones models. This is especially true in the context of nutrient remediation in oligotrophic sub-tropical and tropical habitats that are highly sensitive to small increases in nutrients.

Unlike macroalgae and seagrasses, BMA growth and production is not limited by extreme temperatures or ice cover (Sundback et al. 2000, Glud et al. 2002) even though shallow temperate estuaries can experience large daily and seasonal temperature shifts. Sediment type, tidal exposure, grain size, bottom water velocity, sediment resuspension, and organic matter loading are key drivers of BMA biomass variability in temperate estuaries (Sundback et al. 2000, Thornton et al. 2002), not daily or seasonal temperature variability. The composition of the BMA community changes seasonally in temperate systems, but the function of BMA community remains largely the same. Located at the sediment-water interface, BMA have been shown to function as a filter that prevents the release of sediment-derived nutrients to the water column in temperate estuaries (Krom 1991, Risgaard-Petersen et al. 1994, Sundback et al. 2000). This filtering action can delay or prevent the formation of macroalgal blooms in some systems (Sundback et al. 2000).

Aside from functioning as filter at the sediment surface, BMA can also indirectly alter many nutrient cycling processes. BMA primary production has been shown to alter oxygen penetration into surface sediments (Revsbech et al. 1983, Risgaard-Petersen et al. 1994). and nutrient dynamics at the sediment-water interface (e.g. Krom 1991, Rysgaard et al. 1995, McGlathery et al. 2001) (Fig. 1). Decreased nutrient effluxes from the sediment to the water are often attributed to BMA production, but early studies were not designed to directly measure the effect of BMA production on nutrient fluxes. More recent studies have shown that oxygen production in shallow temperate systems can stimulate nitrogen removal through coupled nitrification-denitrification, if ammonium is available, (Risgaard-Petersen et al. 1994, An & Joye 2001, Dalsgaard 2003) and thereby

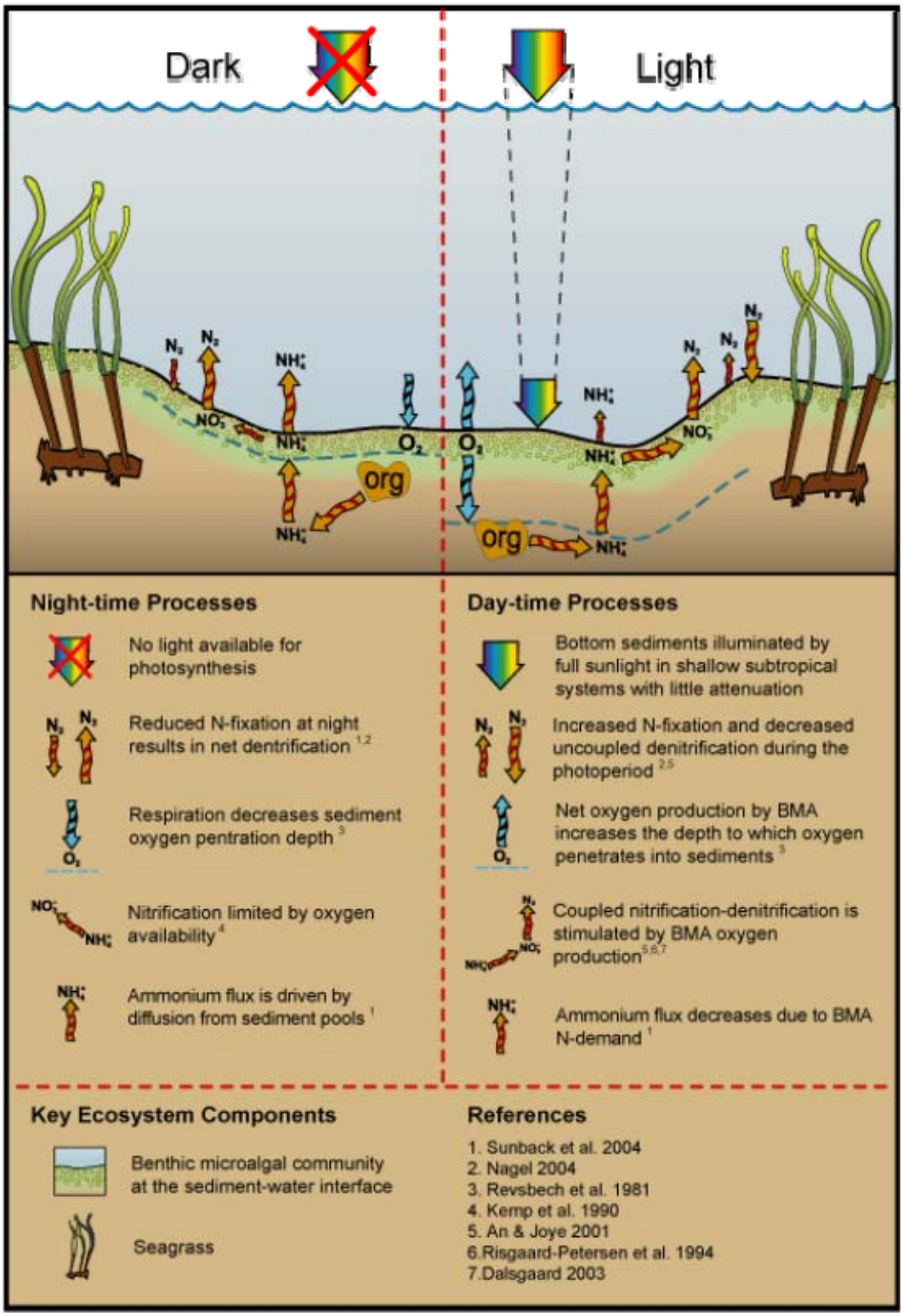

Figure 1. A conceptual diagram of diurnal nitrogen dynamics in the top 5 cm of a BMA-dominated sediment patch in a sub-tropical lagoon.

decrease DIN fluxes to the water column (Dalsgaard 2003, Sundback et al. 2004). Conversely, other studies have shown that primary production inhibits dentrifiers by increasing sediment oxygen concentrations, thereby decreasing nitrogen removal by denitrification (Tiedje et al. 1989, Risgaard-Petersen et al. 1994, An & Joye 2001). Few studies have investigated how BMA primary production, and its effects on nutrient cycling, in a sub-tropical estuary are different than the temperate estuaries from which our knowledge is currently based.

The studies in this thesis used Florida Bay as a representative, shallow, sub-tropical estuary to test the effect of BMA production on N-cycling at the sediment-water interface. BMA in seagrass-free sediments of Florida Bay often receive irradiances greater than 500 μmol photons m^{-2} s^{-1}, unlike temperate systems of similar depth. As a result of increased irradiance, I expected Florida Bay BMA to be more productive in relation to temperate estuarine systems. As in temperate systems, this increased productivity could have either a positive or negative effect on N-cycling.

Multiple sites in Florida Bay were initially surveyed to determine the spatial variability in BMA biomass, production and N-cycling. A second study focused on N-cycling in an extensive and persistent BMA-dominated sediment patch in Sunset Cove, near Key Largo. The objective of this detailed study was to quantify seasonal variability of the effect of BMA oxygen production on nitrogen fluxes within a single sub-basin. Finally, sediment oxygen dynamics related to BMA production were investigated using microelectrodes on Sunset Cove sediments (e.g. Revsbech et al. 1983, Jorgensen & Revsbech 1985, Glud et al. 1992, Kuhl et al. 1996, Berg et al. 2001). I investigated the effects of irradiance on porewater high-resolution oxygen profiles and estimated

photosynthetic oxygen production and community respiration from the profiles (Revsbech & Jorgensen 1983, Berg et al. 1998). All of the present studies were designed to further our understanding on the effects of BMA oxygen production on N-cycling in Florida Bay, a shallow, oligotrophic, sub-tropical estuary.

Methods and Materials

Study Site

Florida Bay is a semi-enclosed, shallow, sub-tropical estuary located off the southern tip of Florida. It is bound to the north by the Everglades and to the east and south by the Florida Keys (Fig. 2). Through out most of the 1900's, dense seagrass and sparse benthic macroalgae were the dominant primary producers in Florida Bay (Zieman et al. 1989). Large-scale seagrass die-off occurred in 1987 and seagrass biomass continued to decline through the 1990's (Robblee et al. 1991, Hall et al. 1999). As a result, there are large sediment patches that are nearly dominated by BMA (Robblee et al. 1991).

The average depth of Florida Bay is ~1 m. It is divided into deeper basins (3-4 m) separated by shallow (<1 m) calcium carbonate mud banks which serve to restrict hydrologic exchange between basins. Freshwater inputs are primarily from Everglades runoff that enters through Taylor Slough in the north central basins of Florida Bay. Despite this freshwater input, hypersaline conditions during the summer are typical through out most of the bay due to restricted exchange between basins (Nuttle et al. 2000). The average annual temperature is 24.5 °C with mean monthly low typically occurring in January and the mean monthly high in August (Fourqurean & Robblee 1999). Seasonal temperature variation in this study ranged from 20 to 32ºC.

Four sites were used in a bay-wide survey to represent the regions of Florida Bay as described in Fourqurean and Roblee (1999). Barnes Key basin (South), Rabbit Key Basin (West), Rankin Bight (North/Central), and Sunset Cove (East) have all experienced

seagrass decline, and have both healthy seagrass beds and seagrass-free sediment patches (Fig 2). Although Florida Bay is generally considered to be oligotrophic, nitrogen and phosphorus water column concentrations in Sunset Cove are slightly elevated and generally attributed anthropogenic sources on Key Largo (Kemp et al. 2001). These four sites were surveyed in June 2003 to quantify the spatial variability of BMA biomass, oxygen, and nitrogen fluxes. Different BMA habitats, within a dense seagrass beds and in a seagrass-free sediment patches, were also examined in each of the sub-basins. Sunset Cove (N 25 05.737, W 80 27.476) was also used for a detailed annual study in 2004 and for source sediments used as a sediment source for the microelectrode porewater profiling.

Experimental Design: Spatial distribution of BMA biomass, production and nitrogen fluxes in Florida Bay

In June 2003, four cores were collected by diver each from within a healthy seagrass bed (Veg.) and from a seagrass-free sediment patch (BMA) at Barnes Key Basin, Rabbit Key Basin, Rankin Bight, and Sunset Cove (Fig 2). Each core consisted of a 15 cm depth of sediment with 15 cm of overlying water (Fig. 3). Cores from within the seagrass beds were collected between vegetative shoots to exclude seagrass biomass. Prior to incubation, the head water of each core was fully exchanged with aerated site water during an overnight dark acclimation period (10-12 h). Within 24 hours of collection, six batch cores (n=3 Veg., n=3 BMA) were sealed and incubated in a tank of site water, at *in situ* temperatures (Fig 3). Two cores containing water only were

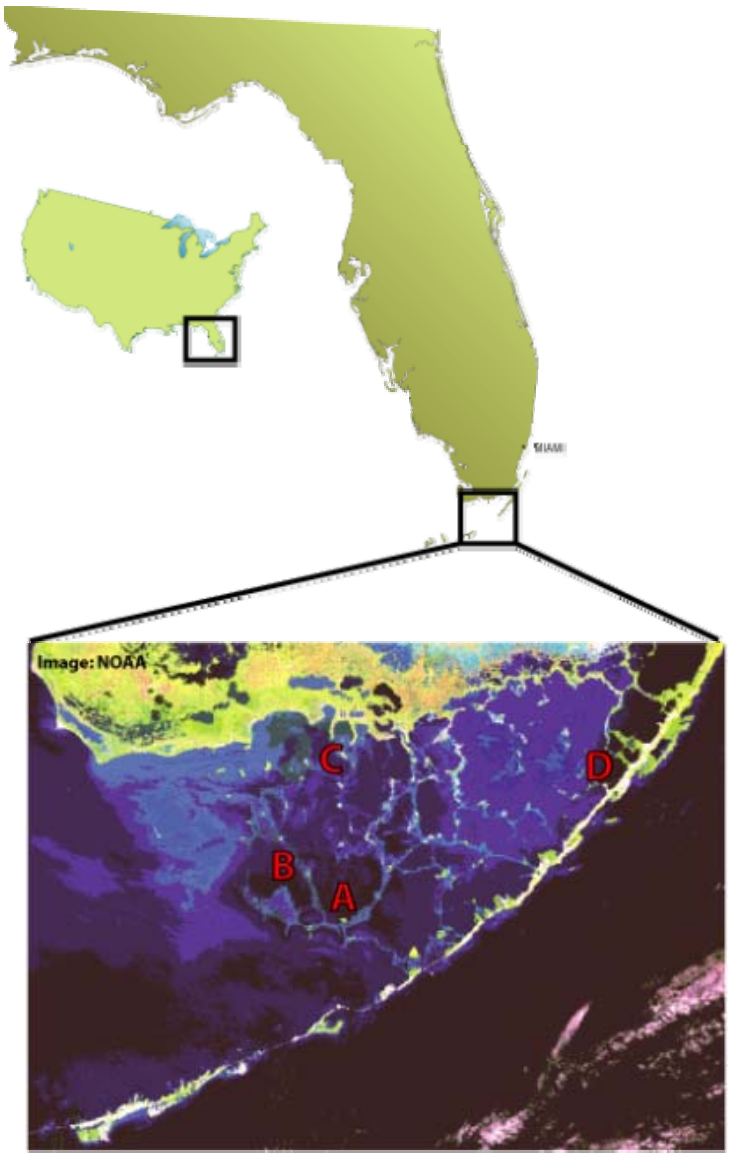

Figure 2. Map of Florida Bay, Florida, bound to the north by the Everglades on the Florida peninsula and to the south and east by the Florida Keys. Four study sites are shown: A) Barnes Key Basin, B) Rabbit Key Basin, C)Rankin Bight, and D) Sunset Cove. Calcium carbonate mud banks (light blue) are visible between the smaller mangrove keys (light green islands) within Florida Bay. (Satellite image of Florida Bay courtesy of NOAA)

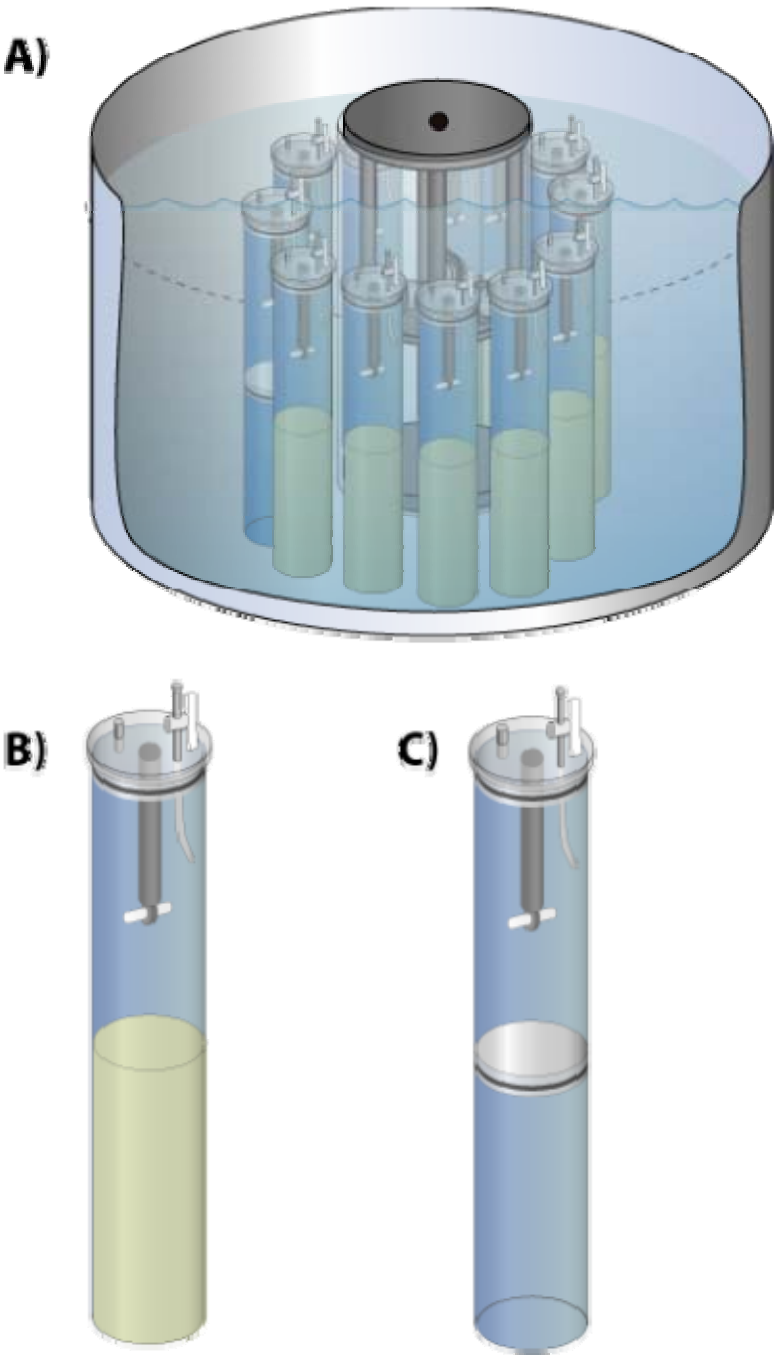

Figure 3. Schematic of A) experimental incubation tank containing sample cores surrounding a central magnetic turntable, and B) a sediment core and C) a water column blank core, each with dual sampling ports in the lid and an internal magnetic stir bar.

incubated simultaneously to quantify water column metabolic activity and used to correct for water column activity in experimental sediment cores.

The cores were incubated for 2-4 hours each under dark and natural sunlight. Dark/light treatments were timed to coincide with natural diel light cycles with dark incubation in the early morning immediately followed by light incubations under ambient natural light. PAR at the sediment surface of experimental cores was continuously monitored for the duration of each experiment with two submersible photosynthetic irradiance recording systems (Dataflow Systems PTY, Ltd.) in the experimental tank. Irradiance during illuminated periods typically ranged from approximately 50 to 2000 μmol photons m^{-2} s^{-1} of natural sunlight. Approximately 40 ml of water was removed at each sampling point, with an equal volume of site water replacing the sample from a head tank such that the cores remained sealed. Samples for dissolved $N_{2(g)}$ and $O_{2(g)}$, NH_4^+, NO_3^- + NO_2^-, and soluble reactive phosphorus (SRP) were collected through sampling ports in the core lids (Fig. 3) every 0.5-1 hour, for a total of four sampling times. Dissolved $N_{2(g)}$ and $O_{2(g)}$ samples were collected in 5 ml glass test tubes free of all air bubbles and preserved with 10 μl 50% saturated HgCl to prevent further metabolic activity. Nutrient samples were collected with a 20 ml syringe, filtered to 0.45 μm, and frozen in 5 ml aliquots for later analysis. Overlying water in each core was mixed using an externally driven magnetic stir bars (~30 rpm) suspended from the core lids during the incubations (Fig. 3).

The extra acclimated cores (1 Veg., 1 BMA) were sectioned for porewater profiles of H_2S, NH_4^+, NO_3^- + NO_2^-, and SRP, and benthic chlorophyll *a* (chl-*a)* at the

start of the incubation period. Following batch core incubations, two cores, one vegetated and one BMA, were randomly selected to be sectioned for the same porewater analysis for comparison. Cores were sectioned at depth intervals of 0-0.5, 0.5-1.0, 1.0-1.5, 1.5-2.0, 2.0-3.0, 3.0-4.0, 4.0-7.0 and 7.0-10.0 cm, and packed in a 50 ml centrifuge tubes under a N_2 atmosphere in a glove bag to maintain anoxic conditions within the sediments. Porewater was separated from the sediments by centrifugation (2500 rpm, 10 min), then filtered (0.45 μm) and frozen for later analysis of NH_4^+, NO_3^- + NO_2^-, and SRP. Prior to freezing, a 1 ml sub-sample of the porewater was fixed with a mixed diamine reagent and stored at room temperature for later sulfide analysis (Cline 1969). Chl-*a* was randomly sub-sampled (10 ml syringe core to 1 cm depth) from each experimental core to estimate of BMA biomass. Chl-*a* samples were stored frozen (-25°C), in the dark, until analyzed with in one month of collection.

Experimental Design: Nitrogen cycing in Sunset Cove, Florida Bay

Sediment cores were collected from Sunset Cove in January, March, June and August 2004. Incubations were done as described previously, in this case to relate nutrient flux rate to photosynthetic oxygen production by BMA during each of the sampling months. Intact sediment cores (n=9) were collected by diver from a BMA dominated sediment patch and acclimated as described previously. Following acclimation, three cores were sectioned for initial porewater characteristics and six cores were incubated in a tank of site water at *in situ* temperatures. Three (15 cm) water column-only cores were incubated as blanks.

To investigate the effects of oxygen production on a diurnal time scale, ambient light conditions for the core incubations were manipulated by covering the cores in either black plastic (dark), or two, one or no layers of neutral density screening. This shading regime resulted in 3 light treatments: 0, <100, and >500 μmol photon m^{-2} s^{-1} of natural sunlight. Again, light treatments were timed to coincide with natural irradiance cycles with the dark treatment at or before sunrise and the shade treatments decreased serially to full ambient irradiance (no screen) at approximately solar noon. The exterior sediment portion of each core was wrapped in aluminum foil and secured with electrical tape at the sediment surface to eliminate light exposure for deep sediments on the circumference of the clear acrylic cores . PAR at the sediment surface of experimental cores was continuously monitored for the duration of each experiment with two submersible photosynthetic irradiance recording systems (Dataflow Systems PTY, Ltd.) in the experimental tank. Full, ambient light readings were verified with independently monitored PAR measurements (Kemp and Cornwell, unpublished data). Cores were incubated at each light level for 1-2 hours with a total incubation time of 6-8 hours. During incubation at each light manipulation, the water column was sampled a minimum of 3 times at intervals of 0.5-1.0 hour with samples for dissolved $N_{2(g)}$ and $O_{2(g)}$, NH_4^+, $NO_3^- + NO_2^-$, and SRP collected in the same manner as previously described.

As in the previous experiment, the three additional acclimated cores were sectioned for initial porewater profiles of H_2S, NH_4^+, $NO_3^- + NO_2^-$, and SRP, and chl-*a* at the start of the incubation period. Following batch core incubations, the six experimental cores were sampled for chl. *a*, and sectioned porewater nutrients (n=3) or sediment bulk density and porosity (n=3). Chl-*a* was randomly sub-sampled (10 ml syringe core to

1 cm depth) from each core as an estimate of BMA biomass. Chl-*a* samples were stored frozen (-25°C), in the dark, and analyzed within one month of collection. Porewater was extracted at the depth intervals as described previously.

Sediment bulk density and porosity were sampled from the three remaining experimental cores at the same depth intervals as the porewater. Wet sediment volume was determined by the gravimetric volume of deionized water added to the wet sediments in a known volume container. Sediments were dried to constant weight at 80°C. Sediment bulk density (ρ) was calculated as grams dry weight of sediment per unit volume. Porosity (φ) was estimated in June and August 2004, as the porewater volume per (total wet sediment volume plus porewater volume). The average porosity at each depth from June and August 2004 was assumed to represent the average porosity at each depth across all sampling dates. The average porosity was used to correct sediment bulk density for salt content assuming that at each date the porewater salinity was equal to the salinity of the overlying water column.

Dissolved gas, nutrient and chlorophyll a *analyses*

Dissolved concentrations were determined using membrane inlet mass spectrometry (MIMS) (Kana et al. 1994, Kana et al. 1998). With this method, high precision $N_{2(g)}$ and $O_{2(g)}$ concentrations are determined relative to the inert gas, argon. N_2:Ar and O_2:Ar ratios were used to detect small concentration changes of N_2 and O_2 relative to Ar during the incubation period. Since changing oxygen concentration during the course of a batch core experiment alters the analytical detection of N_2 and Ar (Eyre et al. 2002), MIMS was calibrated with water samples ranging from 0-100% O_2 saturation

and N_2:Ar ratios were corrected for the oxygen interference (Kana & Weiss 2004). N_2 concentrations were determined based on oxygen corrected N_2:Ar values as described by Kana et al (1998). Dissolved inorganic water column and porewater nutrients (NH_4^+, SRP, $NO_3^- + NO_2$) and hydrogen sulfide were analyzed using standard seawater methods described in Parsons et al. (1984). Benthic chl-*a* samples were extracted in 10 ml 90% acetone for 24 hours at 0°C following 1 hour of sonication. The supernatant was filtered (0.45 μm) and chl-*a* concentrations were determined using HPLC (Van Heukelem et al. (1994).

Oxygen, nitrogen and nutrient fluxes

Oxygen and nitrogen gases, and dissolved inorganic nutrient flux rates were determined by the change in water column concentration between each sampling time. Individual sediment core flux rates were corrected for water column production by subtracting the average (n= 2 or 3) concentration change in cores with water only. All fluxes were normalized to sediment surface area in each core. A positive flux was an efflux from the sediments to the water column, while a negative flux was a flux out of the water column into BMA or the sediments. Fluxes determined by this method represent the net processes across the sediment-water interface.

Net benthic microalgal oxygen production was estimated based on the observed oxygen flux. Oxygen fluxes in the dark were used as an estimate of community respiration (CR_{ox}) and included the net respiration of both BMA and microbial communities. Light oxygen fluxes were used as a measure of benthic net primary production (NPP_{ox}). BMA gross primary production (GPP_{ox}) was calculated as the sum

of NPP_{ox} and CR_{ox}. Daily primary production rates were calculated by extrapolating the observed NPP_{ox} and CR_{ox} hourly rates to daylight (January = 11 h, March = 12 h, June = 14 h, August = 13 h) and dark hours, respectively, in a day.

Net denitrification rates were the measured N_2 (μmol N_2-N m^{-2} h^{-1}) flux rate, corrected for oxygen effects, in all dark incubated cores (Kana et al. 1994, Kana & Weiss 2004). Although N_2-N flux rates were measured during light incubations, they indicate net N-fixation rates that are biologically impossible. These fluxes do not accurately represent net N_2-N fluxes due to gas stripping associated with bubble formation from benthic primary production (Kana, personal communication).

Diffusive NH_4^+ fluxes (J_{sed}) were estimated for all Sunset Cove N-cycling experimental cores. Fick's First Law of Diffusion (eq. 1) was applied to the NH_4^+ concentration in the surface 2 cm of sediment to estimate the hourly diffusive NH_4^+fluxes:

$$J_{sed} = -\varphi \cdot D_{sed} \cdot \frac{\partial C}{\partial z} \qquad \textbf{Equation 1}$$

where φ is the porosity and $\frac{\partial C}{\partial z}$ is the linear concentration gradient in the top 2 cm of sediments. D_{sed} is the diffusivity of NH_4^+, corrected for tortuosity (Boudreau 1997), at the experimental temperature.

Estimating benthic microalgal nitrogen assimilation

Benthic microalgal nitrogen assimilation was calculated as nitrogen demand necessary to support the observed GPP_{ox}. A photosynthetic quotient (PQ) of 1.2 was used to convert GPP_{ox} to GPP_c since PQ was not directly measured in this study

(Sundback & Miles 2000, Wetzel & Likens 2000). Other studies have found a 1.2 ratio of O_2:TCO_2 for arctic sediments (Glud et al. 2002) and 0.23-1.82 for autotrophic sub-tropical sediments (Ferguson et al. 2003). Carbon assimilation (GPP_c) was corrected for autotrophic respiration, assumed to be 10% GPP (Cloern 1987), and N-demand was estimated based on a C:N ratio of 9 (Sundback & Miles 2000). Daily N-demand was calculated by extrapolating the observed hourly N-demand to daylight hours per day (January = 11 h, March = 12 h, June = 14 h, August = 13 h). Dark periods, during which there is no BMA production, were assumed to have no nitrogen demand. This method can underestimate actually BMA nitrogen assimilation because it does not include the potential uptake and storage of N by BMA during dark periods.

Statistical Analyses

For the bay-wide survey on the spatial distribution of BMA biomass and fluxes in Florida Bay, Pearsons linear correlation was used to examine the relationship between the dependent variables, BMA biomass, and $N_{2(g)}$, $O_{2(g)}$ and NH_4^+ fluxes. Spatial variability of BMA biomass and fluxes was tested with a nested ANOVA using site as main grouping variable. Habitat (Veg. vs. BMA) and experimental irradiance (dark vs. light) were the variables used for sub-groups. As there was no treatment effect at the site level, all sites were pooled to compare the effects of habitat and irradiance treatments. Post-hoc multiple pair-wise comparisons were conducted between experimental treatments and interactions using Tukey-Kramer adjusted least square means. For this and all subsequent analyses, differences were accepted at $p<0.05$.

Repeated measures ANOVA, with depth as the repeated variable, was performed on porewater profiles to assess differences between initial and final profiles for each month in Sunset Cove (January-August 2004). No differences were found between initial and final porewater conditions. Initial and final profiles were pooled to a single mean profile to compare differences between months. Multiple pair-wise comparisons (Least Square Means with Tukey-Kramer adjustment) between months were assessed at each depth interval in the porewater profile.

The effect of irradiance on fluxes in Sunset Cove was tested with a 2-way ANOVA using light and experimental date as main factors. Multiple pair-wise comparisons between the means of each light level at each date were tested with least square means (Tukey-Kramer adjustment). All statistical analysis was conducted with SAS 8.2 (SAS Institute).

Experimental Design: Oxygen microelectrode profiling in a controlled light environment

Thirteen sediment cores were collected by diver from Sunset Cove, Florida Bay between two sampling campaigns in late October and early November 2004. Upon collection, the cores were stored in a temporary tank of aerated ambient seawater. Within 24-hours of collection, the cores were sealed, and placed in a small cooler for transportation by air from Key Largo, Florida to Horn Point Laboratory, Cambridge, MD. The corrs arrived at Horn Point Laboratory within 48 hours of collection, and were carefully opened and inspected for disturbance during transportation and for the presence of gastropod grazers immediately upon arrival. Grazers were carefully removed if they were visible on the sediment surface. The sediment portion of the cores was wrapped in

aluminum foil, ~1 mm below the sediment surface, to prevent illumination of the side of the cores. The cores were then gently immersed in a bath of aerated seawater that had been collected previously from Sunset Cove in August 2004. During the acclimation and experimental periods, salinity in the seawater bath was adjusted to, and maintained at ambient salinity with deionized water. The sediment cores were acclimated in an environmental growth chamber at ambient temperature (25-26°C) for 36-48 hours. Since benthic diatoms can exhibit endogenous vertical migrations after collection and acclimation (Pinckney & Zingmark 1991, Mitbavkar & Anil 2004), a natural light cycle was maintained for the duration of the experiment.

The sediment porewater oxygen concentration was profiled with an oxygen microelectrode (OX-25fast Uniscence, Denmark) using a motorized micromanipulator (MM33-M, Uniscence) with 100 μm steps under dark, low and high irradiances (0, 500-700, and 1000-1200 μmol photons m^{-2} s^{-1}, respectively). The microelectrode current was read with a picoammeter and recorded with Profix (v. 3, Uniscence). All profiling was completed under controlled irradiances and temperature in the environmental growth chamber. The cores were acclimated at each light level for 2 hours prior to profiling, and light/dark profiling was timed to correspond with natural irradiance cycles. Each core was profiled individually, in two randomly selected locations at each light level. The sediment-water interface was visually determined with the aide of a magnifying glass (10x). Each profile was started 2000 μm above the sediment-water interface and continued to nearly the maximum depth of oxygen penetration. Profiles were aborted prior to anoxic boundary because the microelectrode tips are easily contaminated by the presence of hydrogen sulfide.

Profile interpretation and oxygen production estimates

Sediment porewater O_2 profiles were interpreted with PROFILE v. 1 (Berg et al. 1998) to determine the depth of maximum oxygen concentration and associated zones of O_2 production and consumption. PROFILE is based on the following one-dimensional mass conservation equation that accounts for molecular diffusion, bioturbation and irrigation:

$$\frac{d}{dx}\left(\varphi\left(D_S + D_B\right)\frac{dC}{dx}\right) + \varphi\alpha\left(C_0 - C\right) + R = 0 \qquad \textbf{Equation 2}$$

where C is the porewater concentration, C_0 is the bottom water concentration, x is depth, φ is porosity, D_S is the molecular diffusivity corrected for tortuosity, D_B is the biodiffusivity, α is the irrigation coefficient, and R is the net rate of production. Concentrations measure with the oxygen microelectrode were used to estimate $\frac{dC}{dx}$. The estimated $\frac{dC}{dx}$, along with known values of φ, D_s, D_B, α, and established boundary conditions (C_0), were then to calculate oxygen production for each sediment volume. In the present study, φ was determined to be 0.96 in the top 0-0.5 cm of sediment and 0.94 from 0.5-1.0 cm sediment depth. Irrigation and bioturbation parameters were ignored ($\alpha=0$ and $D_b=0$) in all PROFILE interpretations. PROFILE creates concentration and production profiles in the sediments through a using two-steps with piecewise-constant functions with uniform production rates in a given sediment zone. In the first step, PROFILE uses the parameterized numerical solution to equation 2 to determine the lowest number of equally spaced depth zones to explain the observed concentration

profile data. The number of zones reduced in the second step, where a series of statistical F-tests to determine if some of the adjacent zones can be combined without losing the quality of fit to the observed data. In this manner, the numerical solution to equation 2 was calculated for each sediment volume of the measured porewater oxygen concentration profile to create a modeled oxygen production and consumption profile.

In this study, each measured porewater oxygen concentration profile was interpreted individually in a two-fold interpretation process. Initially, each profile was interpreted with the boundary conditions of the calculation domain set to be the measured oxygen concentration at the sediment surface and at the maximum depth of the profile. The output of the first interpretation resulted in an estimate of O_2 flux that the top and bottom of the calculation domain. For the second profile interpretation, the boundary conditions were reset to the bottom concentration (as measured) and the bottom flux (as modeled) of O_2. All points were included in the PROFILE interpretation, but outliers were not allowed to determine zone of extreme production or consumptions.

Results

Spatial distribution of water column nutrients, BMA biomass, and oxygen and nitrogen fluxes in Florida Bay

Water column salinity, temperature and nutrient concentrations were similar at all sites within Florida Bay in June 2003 (Table 1). Barnes Key Basin, Rabbit Key Basin, Rankin Bight, and Sunset Cove had salinity range of 32-33 and temperature range of 28-30 °C. Water column NH_4^+ concentrations were low (1.18 – 1.78 μM) at Barnes Key Basin, Rabbit Key Basin and Rankin Bight, and elevated (5.95 μM) at Sunset Cove. SRP in the water column was <0.01 μM at Rabbit Key Basin and Ranking Bight. SRP was low, but detectable, at both Barnes Key Basin and Sunset Cove (0.12 μM and 0.14 μM, respectively). Water column NO_3^- concentrations were not quantified in June 2003.

For both habitat types (BMA and Veg.), there was no significant difference among sites for BMA biomass or fluxes(Appendix 1), and the data for each habitat type were pooled across all sites. BMA biomass was significantly higher in sediment patches without seagrass than in healthy, dense seagrass beds ($p=0.0008$) (Table 2). This habitat difference can also be thought of as a natural treatment factor of high or low BMA biomass. Net sediment oxygen consumption was observed in the dark and net production was observed in the light (Fig. 4). BMA production was significantly higher in seagrass-free sediment patches than in sediments with seagrass present (5674.21 and 722.80 μmol O_2 m^{-2} h^{-1} respectively, $p<0.0001$). Oxygen consumption rates, representing community respiration, were similar in sediments with and without

		Salinity	Temp (ºC)	NH_4^+ (µM)	SRP (µM)	NO_3^- (µM)
Barnes Key Basin	June 2003	33.1	30.1	1.48 ± 0.14 (16)	0.12 ± 0.06 (16)	--
Rabbit Key Basin	June 2003	33.5	30.5	1.18 ± 0.34 (8)	<0.01 (8)	--
Rankin Bight	June 2003	32.8	28.2	1.78 ± 0.51 (8)	<0.01 (8)	--
Sunset Cove	June 2003	32.6	29.9	5.95 ± 0.36 (16)	0.14 ± 0.07 (16)	--

Table 1. Mean water column characteristics ± standard error, n=9 unless otherwise noted by parenthetical value, for each sampling date.

		Benthic Chl a. ($mg\ m^{-2}$)
Barnes Key Basin	BMA	42.5 ± 11.4
	Veg.	6.0 ± 1.9
Rabbit Key Basin	BMA	26.9 ± 14.7
	Veg.	8.5 ± 0.4
Rankin Bight	BMA	27.9 ± 10.0
	Veg.	6.8 ± 0.9
Sunset Cove	BMA	23.3 ± 4.1
	Veg.	10.0 ± 1.9
Mean of all sites	BMA	30.2 ± 5.1 (12)
	Veg.	7.8 ± 2.7 (12)

Table 2. Mean BMA biomass ± SE (n=3 unless noted) for each habitat sampled, seagrass-free patches and within dense, healthy seagrass beds, at each site in June 2003.

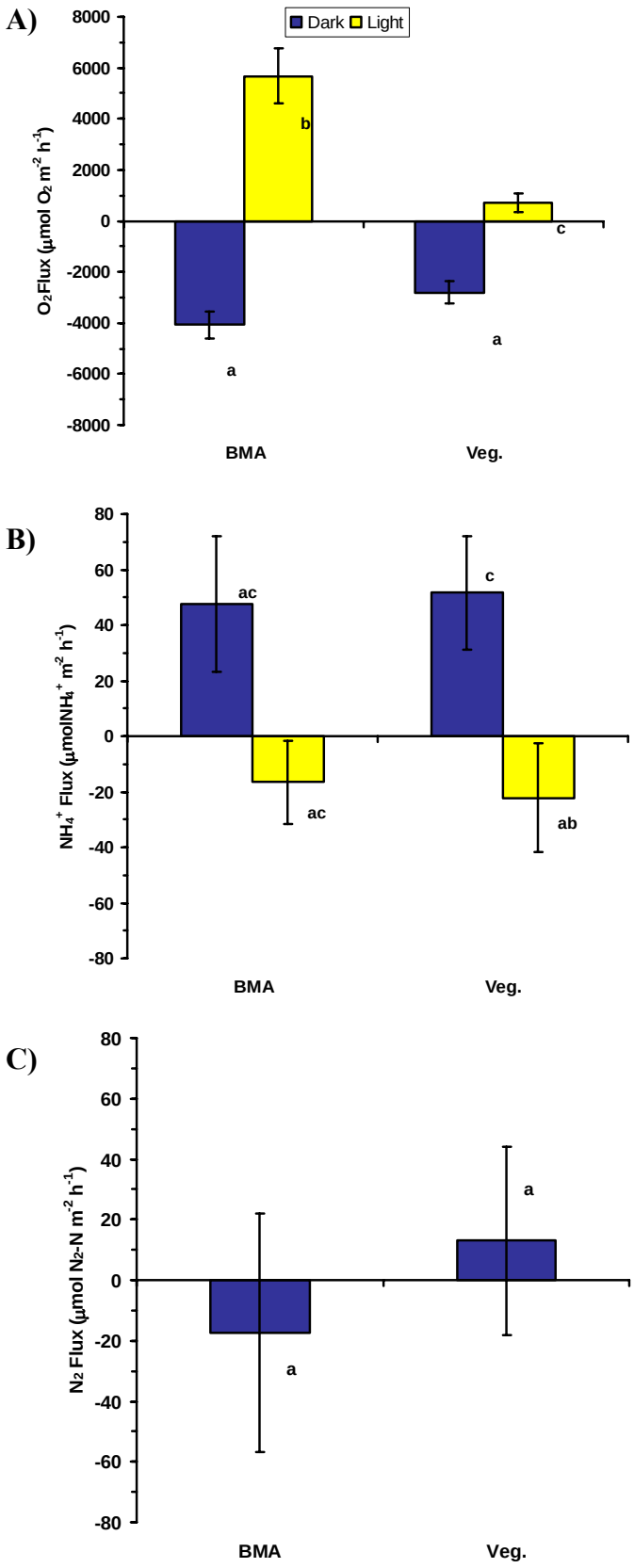

Figure 4. Net sediment fluxes, pooled across sites, within habitat type for a) net oxygen flux, b) net ammonium flux, and c) net denitrification (dark only). Error bars represent the standard error (n=12) and bars with different letters are significantly different from each other (α=0.05). Individual flux measurements are presented in Appendix 1.

seagrass present (-4077.78 and -2799.49 μmol O_2 m^{-2} h^{-1} respectively). BMA biomass was also positively correlated with oxygen production during illuminated incubations ($p<0.0001$, Fig. 5).

Similarly, both habitats displayed a net NH_4^+ release (47.74 - 51.62 μmol NH_4^+ m^{-2} h^{-1}) from the sediments during dark periods and net NH_4^+ uptake (-16.58 to -22.16 μmol NH_4^+ m^{-2} h^{-1}) by the sediments during light periods (Fig. 4) although light NH_4^+ fluxes are not significantly different than zero. Dark sediment oxygen fluxes (community respiration) were positively correlated with NH_4^+ release, suggesting heterotrophic remineralization of organic matter. Concentrations of SRP and NO_3^- + NO_2^- were at or below the analytical detection limit (0.01 μM) and fluxes could not be calculated. Dark denitrification rates, as indicated by the net N_2-N fluxes, were small, not significantly different between seagrass or seagrass-free sediment habitats (13.01 and -17.28 μmol N_2-N m^{-2} h^{-1}, respectively), and were not significantly different from zero (Fig. 4). Vertical profiles of mean porewater nutrient concentrations reveal clear differences between sediments with and without seagrass when pooled across sites (Fig. 6, Appendix 2). Seagrass-free sediment patches had higher porewater H_2S, NH_4^+ and SRP concentrations and more distinct gradients in the surface sediments than those from dense seagrass beds. Analytical interference by H_2S prevented the determination of porewater NO_3^- concentrations.

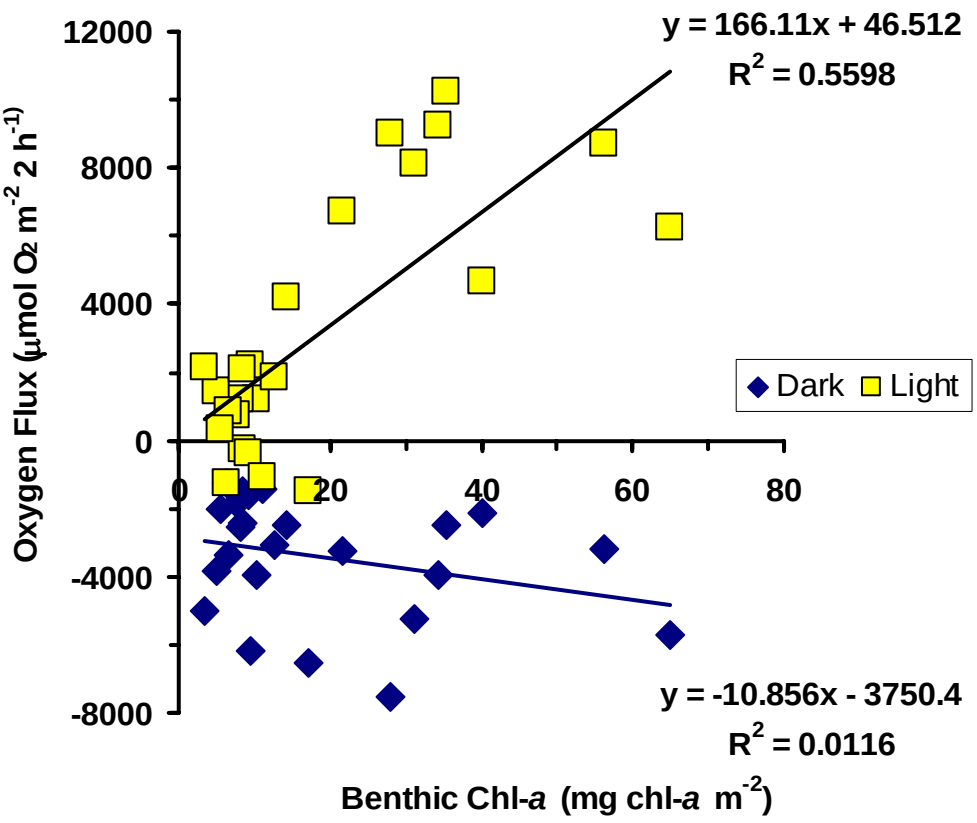

Figure 5. The correlation between mean oxygen flux and BMA biomass, as measured by benthic chl-*a*, during light and dark periods. There is a strong positive correlation between BMA biomass and net oxygen production during illuminated periods. Dark rates of oxygen consumption are not significantly correlated with BMA biomass.

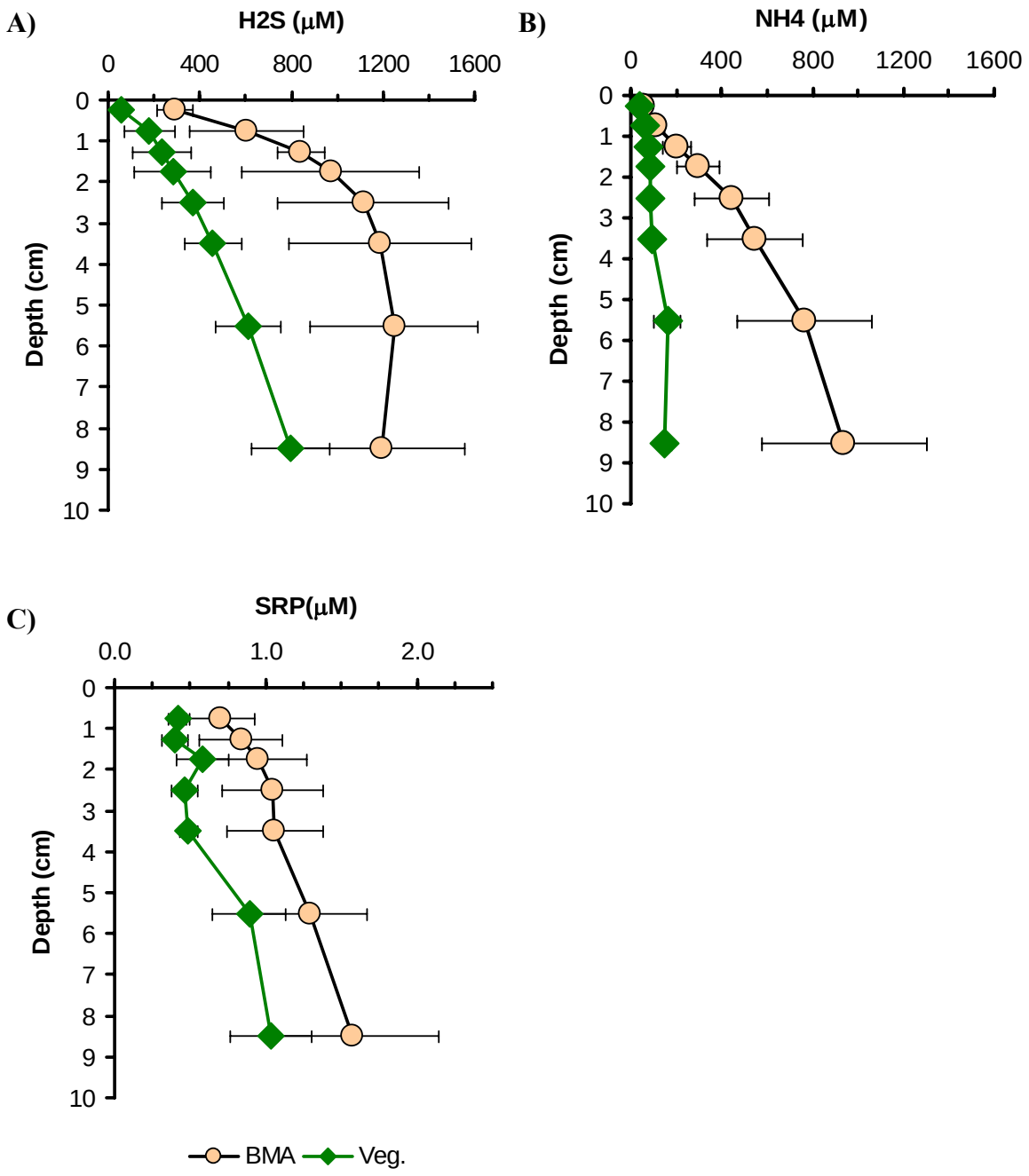

Figure 6. Mean porewater characteristics for a) hydrogen sulfide, b) ammonium, and c) soluble reactive phosphorus between seagrass (Veg.) and seagrass-free (BMA) patches. Porewater concentrations are averaged across all sites, data from individual cores is presented in Appendix 2.

BMA biomass and sediment characteristics in Sunset Cove

Benthic microagal biomass ranged from 24.5-110 mg chl-*a* m^{-2}, with an annual mean of 58 mg chl-*a* m^{-2}, over all experiments in Sunset Cove during 2004 (Table 3, Appendix 3). The highest standing stock of BMA biomass was observed in June, but there was no significant difference in the BMA biomass present during January, March, and June. Several days of sustained winds associated with the passing of Hurricane Charley over southern Florida resulted in low benthic chl-*a* values in August 2004. If the mean BMA biomass from January, March and June is assumed to represent undisturbed conditions, it would appear that hurricane disturbance significantly reduced BMA biomass (α=0.05, p=0.0027). The effects of sediment resuspension in August were also reflected in elevated water column NH_4^+ concentrations (Table 3). Resuspension of surface sediments would have mixed the high nutrient porewater with the nutrient deplete water column. The near-vertical gradient for all porewater nutrient profiles in August also suggests porewater flushing was forced by hurricane-related turbulence (Fig 7).

There was no significant difference between pre- and post-incubation porewater profiles or H_2S, NH_4^+, and SRP for each sampling date (Appendix 4), and all profiles from a given date are presented as a mean profile (Fig. 7). H_2S concentrations range from 73-100 μM in the surface 2 cm of sediments and increased substantially with depth. There was a significant difference between January and March (p=0.009), August and March (p=0.0004), and August and June (p=0.0374) in H_2S concentrations at 7-10 cm depth. The differences may be attributed to exchange of anoxic porewater with oxygenated bath water around the bottom stopper during the experimental incubation or to H_2S oxidation during the core slicing process. As a core was prepared for porewater

	Salinity	Temp (ºC)	Benthic Cal.-*a* (mg chl-*a* m^{-2})	NH_4^+ (μM)	SRP (μM)	NO_3^- (μM)
						1.89 ± 0.07
January	26	20	60.7 ± 8.9 (9)[ab]	4.27 ± 0.50	0.26 ± 0.06	(9)
March	30	21.9	63.6 ± 10.1 (9)[ab]	3.98 ± 0.24	0.20 ± 0.03	1.34 (2)
June	35.8	31.2	74.7 ± 8.6 (9)[a]	2.79 ± 0.20	0.24 ± 0.03	0.94 (2)
August	40.9	31.1	38.3 ± 4.3 (11)[b]	7.91 ± 1.43	0.02 ± 0.02	2.58 (2)
January-June			66.3 ± 5.2 (27)[a]	3.68 ± 0.24 (18)	0.23 ± 0.02 (18)	1.66 ± 0.11 (13)

Table 3. Salinity, temperature, BMA biomass, and water column nutrients on each sampling date in Sunset Cove. Benthic biomass and water column nutrients are presented as the mean ± standard error, n=6 unless otherwise denoted by parenthetical value. The mean benthic biomass and water quality parameters for January, March, and June represent undisturbed conditions, while August reflects wind-driven disturbance from hurricane Charley. Different letters represent statistical difference between the means (α=0.05).

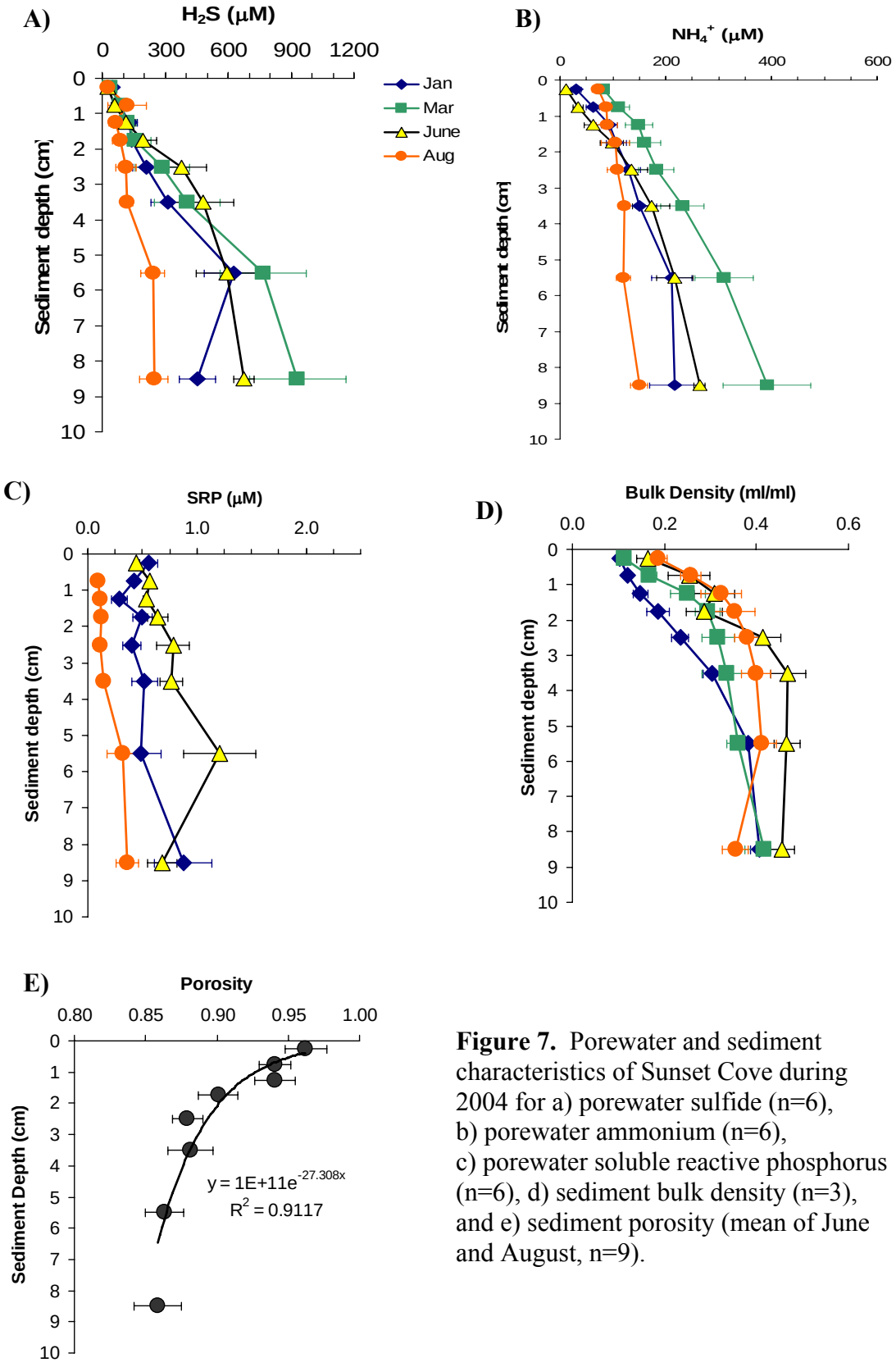

Figure 7. Porewater and sediment characteristics of Sunset Cove during 2004 for a) porewater sulfide (n=6), b) porewater ammonium (n=6), c) porewater soluble reactive phosphorus (n=6), d) sediment bulk density (n=3), and e) sediment porosity (mean of June and August, n=9).

extraction, the bottom incubation stopper was replaced with a smaller rubber stopper, used to extract the core. During the stopper exchange process, the bottom portion of the sediment core was exposed to oxic conditions and some porewater may have been lost. The oxidation of H_2S during preparation of the sediment core for slicing should be taken into consideration when looking at profiles below 7 cm depth.

Sediment porewater concentrations of NH_4^+ also display a pattern of increasing concentration with depth (Fig. 7). In the surface sediments (0-0.5 cm), January is significantly different from March and August ($p=0.0013$ and 0.0072, respectively) as is June ($p<0.0001$ and 0.0003, respectively). March NH_4^+ concentrations were consistently higher than other months at all depths and were significantly different than August below 4 cm depth ($p=0.0091$ at 4-7cm and $p=0.0058$ at 7-10cm), and from January below 7 cm ($p=0.0487$). Porewater SRP profiles were more difficult to interpret due to analytical detection limits. Observed concentrations of phosphorus were near the analytical detection limit (0.01 μM), and it was difficult to determine if the variability shown in the January and June profiles was a true signature of the porewater or if it was an artifact of the analytical method. No data are available for March.

The bulk density of Sunset Cove sediments was very low in the surface sediments and increased with depth (Fig. 7). Overall, the sediment bulk density profiles were very similar between sampling dates (Appendix 4), with slight significant differences occurring at 0.5-1.0 cm between January and August ($p=0.0421$), and at 2-3 cm between January and June ($p=0.0496$). Sediment porosity was only measured in June and August and the mean porosity at each depth interval, from these dates, was assumed to be the average sediment porosity for all experimental dates at Sunset Cove (Fig. 7). This is a

reasonable assumption considering the similarity in sediment bulk density between experimental dates. The surface layer (0-0.5 cm) was 96% water, and characterized by loose, easily resuspended material. Sediment porosity decreased by 10% with depth, and the bottom portion (7-10 cm) of the cores has an average porosity of 0.86.

Oxygen fluxes and production in Sunset Cove

Oxygen fluxes across the sediment-water interface were related to BMA primary production and community respiration. There was a significant effect of light on the oxygen flux, with the BMA community becoming net autotrophic at the onset of illumination in January, March and August (Fig. 8). NPP_{ox} at high light levels in August (2886 μmol O_2 m^{-2} h^{-1}) was significantly less than the mean high light production observed in January, March and June (6714, 7868, and 7659 μmol O_2 m^{-2} h^{-1}, p=0.0003, <0.0001, and <0.0001 respectively). Oxygen fluxes normalized to benthic chl-*a* (Fig. 9) are not significantly different from each other at high light, showing that production per unit BMA biomass is uniform. Estimating the daily oxygen flux from these experiments was a useful indicator of net heterotrophy or autotrophy for the BMA community. GPP_{ox} was highest in March at low light levels and in June at high light levels (Table 4). When irradiances were greater than 500 μmol photon m^{-2} s^{-1} (High Light), the BMA community was always found to be net autotrophic (2 – 61 mmol O_2 m^{-2} h^{-1}). The BMA community was also net autotrophic with light levels less than 100 μmol photon m^{-2} s^{-1} (Low Light) in the winter and early spring (1.8 and 11.5 mmol O_2 m^{-2} h^{-1}, respectively) but net

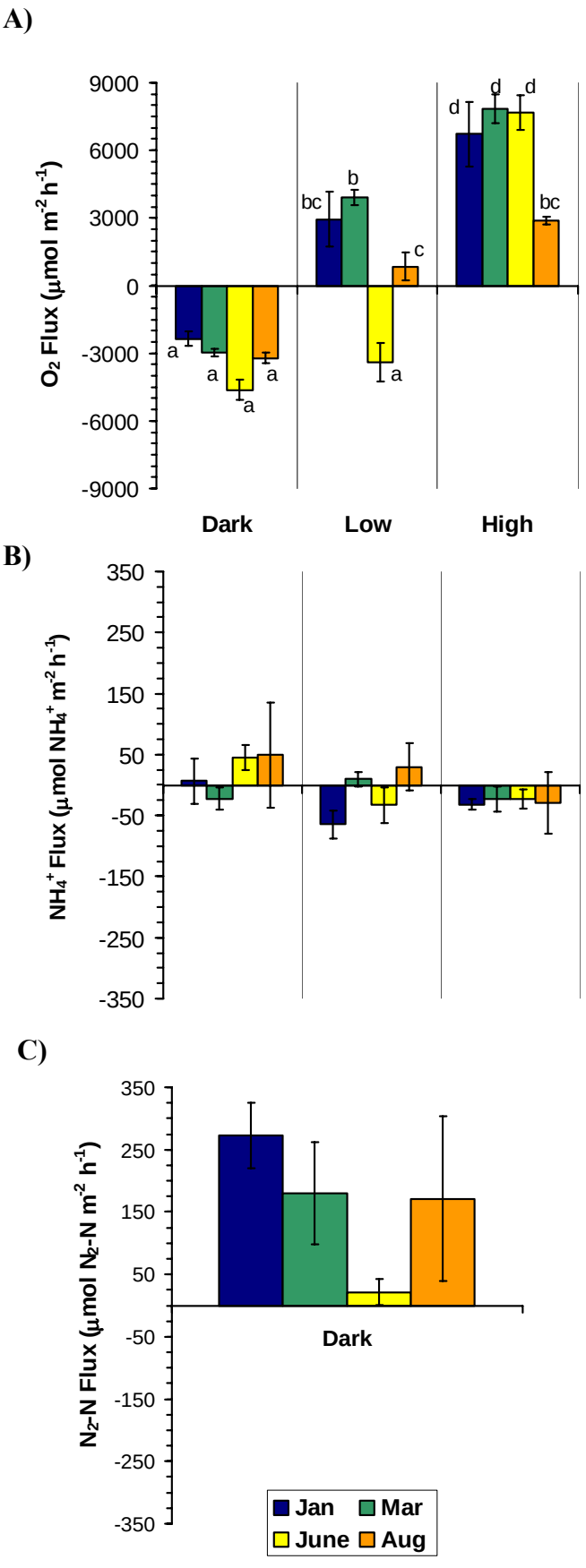

Figure 8. Net sediment fluxes for a) oxygen, b) ammonium, and c) denitrification (dark only) Error bars represent the standard error (n=5-6). The letters represent a significant difference between fluxes (α=0.05). There is no significant difference between ammonium fluxes or denitrification.

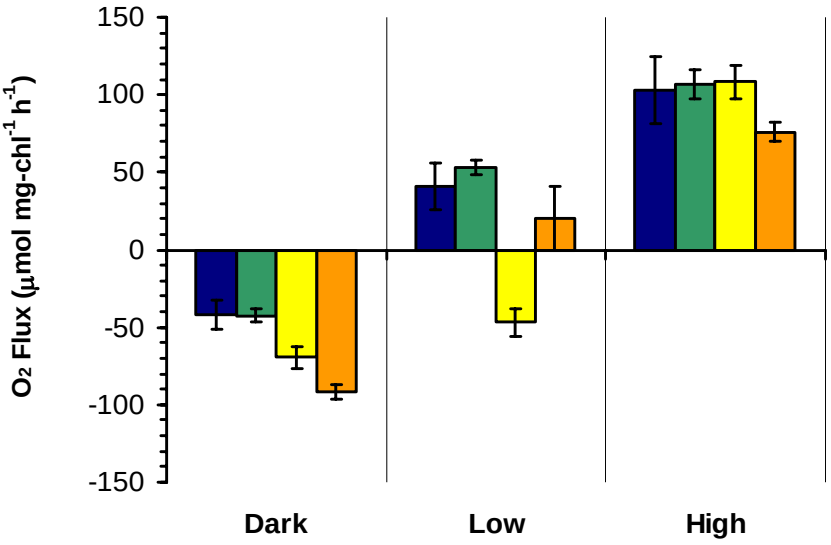

Figure 9. Oxygen fluxes normalized to benthic microalgal biomass in each experimental core. At high light levels, there is no significant difference in oxygen production per unit chlorophyll.

	Light	January	March	June	August
Community Respiration ($\mu mol\ O_2\ m^{-2}\ h^{-1}$)	Dark	2334 ± 321	2792 ± 167	5008 ± 443	3410 ± 298
Net Primary Production ($\mu mol\ O_2\ m^{-2}\ h^{-1}$)	Low	2906 ± 1222	4105 ± 654	-3706 ± 854	-183 ± 834
	High	6611 ± 1442	8062 ± 642	7348 ± 770	2059 ± 241
Gross Primary Production ($\mu mol\ O_2\ m^{-2}\ h^{-1}$)	Low	5240 ± 1380	6896 ± 690	1301 ± 552	3202 ± 685
	High	8944 ± 1515	10854 ± 685	12356 ± 855	5444 ± 337
Daily Oxygen Flux ($mmol\ O_2\ m^{-2}\ d^{-1}$)	Low	1.80	11.45	-93.63	-24.49
	High	43.21	47.82	61.02	2.04

Table 4. Values represent mean ± SE for community respiration (CR), and net primary production (NPP_{ox}), gross primary production (GPP_{ox}) at each light level. Community respiration is assumed to be constant at all light levels. Mean daily oxygen fluxes are normalized for hours of daylight during each sampling period, assuming either low or high light for the entire daylight period.

heterotrophic during summer and early fall (-93.6 and -24.5 mmol O_2 m^{-2} h^{-1}, respectively) (Table 4). Low net production, at both low and high light levels, in August was due to low BMA biomass from hurricane-related disturbance.

Nutrient fluxes and BMA nitrogen demand in Sunset Cove

Fluxes of dissolved inorganic nutrients could not be calculated for all analytes. Water column NO_3^-/NO_2 and SRP were at or near the analytical detection limits (0.01 μM) for the duration of most of the incubations, making detection of concentration changes difficult. Changes in water column NH_4^+ concentration were detectable and fluxes were calculated (Fig. 8). The mean observed NH_4^+ fluxes were not significantly different from each other or from zero, partially due to high variability between cores at each light treatment. Under high light conditions more of the individual cores displayed negative fluxes, as would be expected from increased NH_4^+ uptake by BMA with higher production rates. Observed dark NH_4^+ fluxes in August were larger than in previous months while the porewater NH_4^+ profiles indicated a small concentration gradient in the top 10 cm (Fig. 7). This is consistent with what would be expected following a disturbance event, such as sustained winds from a hurricane.

Nitrogen demand during illuminated periods was calculated for both low and high light conditions (Table 5). Either consistent low light or high light rates were assumed to be constant for the average daylight hours per day of each month. For example, daily N-demand of BMA under low light conditions in January was estimated as the hourly rate multiplied by 11 hours of illumination per day. Nitrogen demand on an hourly basis increases by 35-41% between low and high light, with the exception of June where the

	Light	January	March	June	August
Diffusive NH_4^+ Flux (mmol m^{-2} d^{-1})		0.62	0.67	0.88	0.33
Observed NH_4^+ Flux (mmol m^{-2} d^{-1})	Low	-0.63	-0.15	-0.01	0.93
	High	-0.27	-0.54	0.12	0.17
N-demand (mmol m^{-2} d^{-1})	Low	4.80	6.90	1.52	4.21
	High	8.20	10.85	14.42	6.46

Table 5. A comparison of daily predicted and observed NH_4^+ fluxes with the estimated daily N-assimilation by BMA. Diffusive NH_4^+ fluxes were assumed to be constant for a 24-hour period. The daily observed NH_4^+ fluxes were estimated the average flux rate from dark and low or high light, normalized to the respective hours of dark and daylight.

BMA N-demand increases by 89% between low and high light. Daily BMA N-demand was lowest in June (1.5 mmol NH_4^+ m^{-2} d^{-1}) when GPP_{ox} was lowest under low light conditions. Maximum BMA N-demand was during high light conditions in March and June (10.9 and 14.4 mmol NH_4^+ m^{-2} d^{-1}, respectively) when GPP_{ox} was highest.

Diffusive NH_4^+ fluxes were estimated as a function of porewater NH_4^+ concentrations in the top 2 cm of sediments and with an average porosity of 0.94. Based on these conditions, a diffusive efflux of NH_4^+ from the sediments ranging from 13.8 to 36.8 μmol NH_4^+ m^{-2} h^{-1} should have been observed. On a daily scale, assuming a constant diffusive flux at the estimated hourly rate, 0.33 to 0.88 mmol NH_4^+ m^{-2} d^{-1} could have been released from the sediment by diffusive flux alone (Table 5). The estimated diffusive releases of NH_4^+ were much greater than the observed NH_4^+ flux, suggesting that the diffusive flux was intercepted by the BMA to suppport a portion of the its N-demand. Surface regeneration of NH_4^+, at very fine scales, therefore can provide a portion of the N necessary to support the observed rates of production.

Denitrification in Sunset Cove Microelectrode oxygen profiles

Denitrification, estimated from dark incubations, displayed seasonal variability in 2004 (Fig. 8). The lowest denitrification rates in Sunset Cove were observed in June (21.6 ± 20.4 μmol N_2-N m^{-2} h^{-1}), and were similar to the denitrification rates observed through out Florida Bay in June 2003 (Fig. 4). Denitrification rates in January, March and August 2004 (272.7 ± 53.1, 180.0 ± 82.7, and 171.2 ± 132.1 μmol N_2-N m^{-2} h^{-1}, respectively) were an order of magnitude greater than those observed in both June 2003

and June 2004. Although denitrification in June was much lower than other months, there was no significant difference between the monthly mean denitrification rates. When the dark denitrification rates were extrapolated to a daily denitrification, with the assumption that the observed dark rates were constant over a 24 h period, estimates for January, March and August range from 4.11 to 6.55 mmol N_2-N m^{-2} d^{-1}. Estimated daily denitrification in June was much lower (0.52 mmol N_2-N m^{-2} d^{-1}). However, estimating daily denitrification under this assumption can overestimate denitrification during illuminated periods because it does not account for competition between BMA and denitrifying bacteria for nitrogen substrates.

Microelectrode oxygen profiles

To compare oxygen concentration and rates of production and consumption, the individual profiles were pooled into a single, composite porewater oxygen profile for each light treatment (Fig. 10). Despite variability within and between individual profiles in experimental cores, modeled porewater oxygen concentrations agreed with observed data. Variations in the total depth of oxygen penetration result in 'bumps' in the compilation profiles where there were large changes in the profile slope and oxygen concentrations. Although these features were not observed in the individual profiles (Appendix 5), they were not excluded when interpreting the compilation profiles. Rather, the modeled composite profiles estimated a smoothed concentration gradient which was then used to estimate rates and zones of oxygen production and consumption (Fig 10).

Porewater oxygen concentrations increased with irradiance in the observed and modeled data. In dark periods, maximum oxygen concentrations were at the sediment

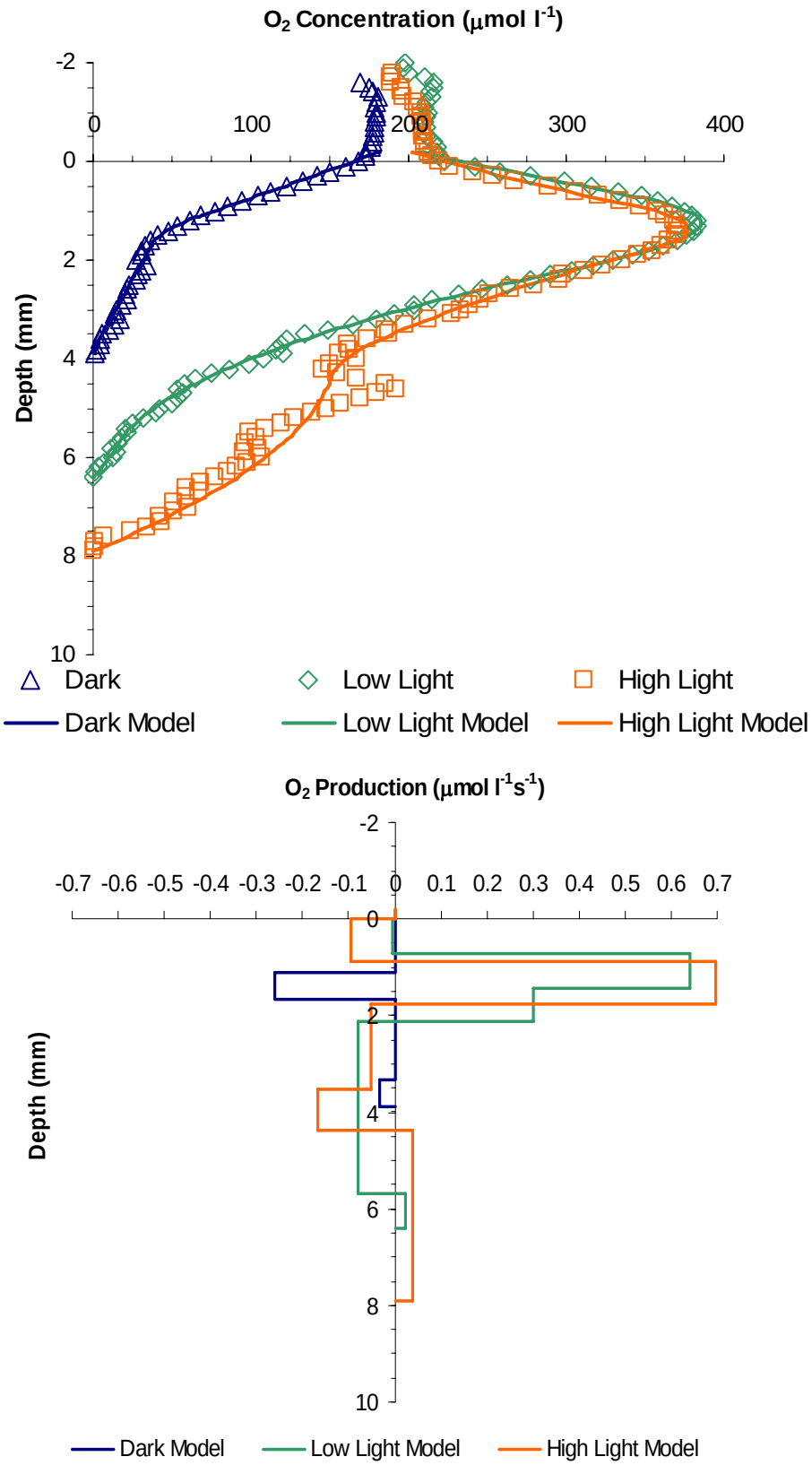

Figure 10. Observed (symbols) and modeled (lines) compilation profiles of porewater oxygen concentration and production in the surface sediments of Sunset Cove.

surface and were similar to water column oxygen concentrations. BMA primary production clearly increased the porewater oxygen concentrations under low irradiance (500 μmol m^{-2} s^{-2}), where the average maximum oxygen concentration was 385 μM at 1.2 mm below the sediment-water interface. Similarly, in high light conditions (1000 μmol m^{-2} s^{-2}), the maximum oxygen concentration was 377 μmol l^{-1} at 0.14 cm depth (Fig. 10). Peak oxygen consumption in the dark and peak production under low and high irradiances occurred in a narrowly constrained zone 0.7-1.7 mm below the sediment surface (Fig. 10).

Oxygen fluxes at the sediment surface were substantially less than those observed with previous flux experiments when estimated from the sediment O_2 profiles (Fig 11). Microelectrode determination of primary production in sediments can be underestimated in sediments with high rates of bubble formation (Revsbech et al. 1981, Revsbech & Jorgensen 1983). Field observations of floating mats of BMA in Sunset Cove, as well as high productivity, suggest that high rates of bubble formation were a common occurrence at the sediment surface. Flux rates observed in batch core incubations integrated oxygen production and consumption of the entire sediment column, and a net flux across the sediment-water interface is observed over several hour incubations. On the other hand, flux rates estimated from modeled concentration profiles are extrapolated from fine-scale spatial and temporal measurements. Large scale processes of bioturbation and bioirrigation were initially ignored in the flux rate calculation and therefore excluded when fluxes were extrapolated to the sediment patch scale. Oxygen flux rates modeled from microelectrode oxygen profiles underestimate next oxygen fluxes across the sediment-water interface in comparison to flux rates observed in batch core experiments.

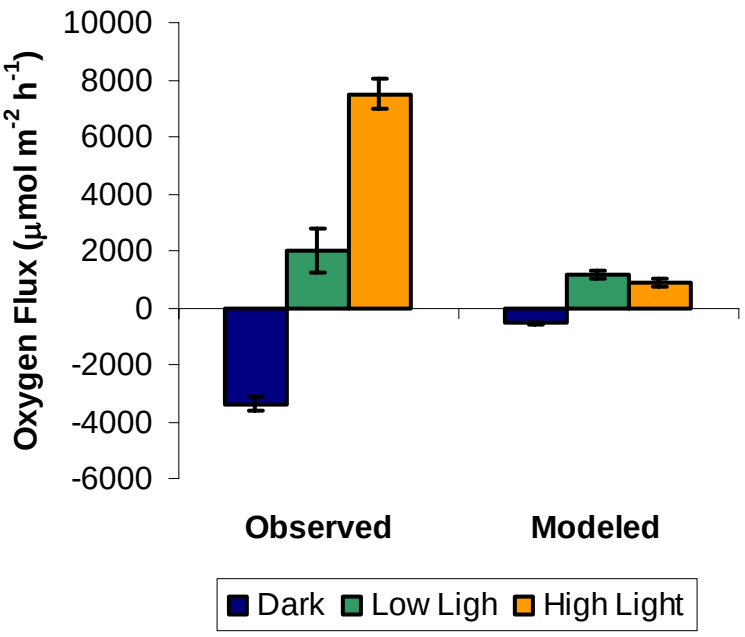

Figure 11. Oxygen flux rates across the sediment-water interface observed in batch core incubations (n=27) (observed) and modeled from microelectrode porewater oxygen concentration profiles (n=13) (modeled). Error bars represent standard error. In the observed fluxes, low light is irradiances <100 µmol photons m^{-2} s^{-1} and high light is >500 µmol photons m^{-2} s^{-1} of natural sunlight. The modeled fluxes are based on porewater oxygen profiles collected under artificial light for low and high intensities of ~500 µmol photons m^{-2} s^{-1} and 1000 µmol photons m^{-2} s^{-1}, respectively.

Discussion

Methods – Estimating denitrification during periods of primary production

There are several methods by which denitrification has been estimated in submerged sediments. Acetylene block, isotope-pairing, direct N_2, N_2:Ar ratios, and stochiometric balance have all been used to estimate dark dentrification rates in a diversity of marine and estuarine environments (see Cornwell et al. 1999 for review). N_2:Ar ratios specifically, as measured with membrane inlet mass spectrometry, have been used to estimate denitrification rates in many different kinds of environments – including estuarine and marsh sediments with and without macrophytes, and aquaculture waste water – but primarily under dark conditions (e.g. Kana et al. 1998, McCarthy & Gardner 2003, Poe et al. 2003, Gardner et al. 2005). This study attempted to estimate denitrification by applying the MIMS technique to illuminated sub-tropical sediments. We found that, once illuminated, N_2-N fluxes in most cores indicated net $N_{2(g)}$ loss, with loss rates ranging from moderate (~1 μmol N_2-N m^{-2} h^{-1}) to impossibly large (~2600 μmol N_2-N m^{-2} h^{-1}).

A plausible explanation of $N_{2(g)}$ loss is the gas stripping effect from the presence of bubbles inside the sealed experimental cores. The supersaturation of oxygen, as a result of BMA primary production, is likely to have resulted in the creation of microbubbles in the cores. As a subsequent result, dissolved gases would have diffused in to the microbubbles and given the same signal as N-fixation or dissolved gas loss from the water column (Kana, personal communication). I attempted to correct for degassing by using the measured changes in dissolved Ar concentrations to estimate bubble volume

and solubility ratios to estimate the volume of N_2 stripped in each core (adapted from Blicher-Mathiesen et al. 1998). The bubble approximation correction used did not correct the illuminated N_2-N flux rates to biologically expected rates and nor does it account for the loss of $N_{2(g)}$ that was observed. (Appendix 3)

In this study, experimental oxygen concentrations during high light periods exceeded the calibration range of MIMS and results presented here might actually represent an underestimation of primary production. But, changes in oxygen concentrations were large during the incubation period in comparison with initial dissolved gas concentrations, and primary production would not have been underestimated until the experimental cores became saturated with respect to dissolved gases. Using the MIMS method to estimate primary production simultaneously with denitrification is a reasonable and cost effective approach when changes in dissolved gas concentrations can be easily detected. Further experimentation is needed to determine the effectiveness of MIMS at measuring small changes in dissolved gases against a large background concentration, such as with $N_{2(g)}$, when total gas concentrations are supersaturated with respect to temperature and salinity. The dark denitrification rates measured in this study were extrapolated daily rates from dark measurements, assuming equal rates in the light and dark. These extrapolated rates estimate maximum daily nitrogen removal, but may overestimate true denitrification because of possible inhibition of nitrification in the presence of sulfide and by competition between denitrifying bacteria and BMA, and must be interpreted with caution.

Methods – Microelectrode profiling

Accurate determination of the sediment-water interface is a common problem in the application of microelectrodes for sediment profiling, but accurately locating the sediment-water interface is imperative to the interpretation of porewater oxygen profiles (Jorgensen & Revsbech 1985). In the present study, the sediment-water interface was visually determined with a post-hoc adjustment to the location sediment surface as necessary. The post-hoc adjustment of the sediment surface was conduction on individual profiles such that the sediment-water interface was assumed to be at the shift in oxygen concentration gradient (Glud et al. 1994). With this adjustment, the interpreted profiles likely included both the sediment oxygen profile and the diffusive boundary layer—which can exceed 1 mm above the sediment surface in low flow conditions (Jorgensen & Revsbech 1985). The respiration observed in the top 0.07 cm of experimental cores under illumination may be accounted for if the diffusive boundary layer was included in the interpretation. Although the sediment-water interface could not be precisely determined, the sediment surface location presented here is the best available approximation.

BMA primary production in Florida Bay

Benthic microalgal production and nutrient cycling are tightly linked in Florida Bay with benthic chl.-*a* and oxygen fluxes being significantly correlated in both seagrass beds and sediment patches free of seagrass. BMA biomass (Table 2) and net benthic oxygen production were in seagrass beds was, on average, 25% and 87% less than in

seagrass-free sediment patches. Although seagrass-free sediments had higher BMA biomass and oxygen production, NH_4^+ fluxes were similar in both habitats. This suggests that BMA biomass drives differences in production, and subsequently nutrient fluxes, between the two habitats rather than site-scale differences in environmental factors such as currents, carbon availability or nutrient input and regeneration. The availability of labile organic matter is important to consider in relation to nutrient availability, both in support of primary production through mineralization and for removal by denitrification. Seagrass and mangrove detritus was observed in sediments both with and without seagrass, as dead leaves were transported from on habitat to another. Similarly, BMA were observed form mats that float to the sediments surface during periods of high productivity due to bubbles trapped within the mat. The floating BMA mats are hypothesized to a vector to return labile organic matter to seagrass beds. Mineralization of BMA derived organic matter is an internal source of NH_4^+, and potentially dynamic between seagrass beds and sediment patches. In the present study, the sample size was too small to detect site-specific variation beyond the variation expressed in the experimental treatment of sediments with or without seagrass. Armitage et al. (2005) found that seagrass and epiphytes production was related to nutrient availability in Florida Bay but there was no general pattern between sites through out Florida Bay.

In the seagrass-free sediment patches of Sunset Cove BMA biomass is a strong driver of benthic primary production. Rather than changes in seasonal factors, such as temperature, salinity, or irradiance, a large-scale disturbance event had the largest impact on standing stocks of BMA biomass. Benthic microalgal production in temperate estuaries tends to follow the accumulation and decline of BMA biomass on an annual

basis (Pinckney & Zingmark 1993). Florida Bay, on the other hand is sub-tropical and there is little change in BMA biomass on an seasonal basis with sediments free of seagrass having consistently higher BMA biomass than when seagrass is present (Table 3). This is similar to shallow temperate systems where sediment type, and the associated susceptibility to physical disturbance, rather than seasonal factors control BMA biomass (Sundback et al. 1990, Sundback et al. 2000, Thornton et al. 2002, Sundback et al. 2003). In areas free of seagrass, surface sediments in Florida Bay are more easily resuspended by events that cause high shear stress, such as sustained high winds, and disturb the BMA community (Krenn 2003). Despite biomass loss, there was no annual variation in BMA production when normalized per unit chl.-*a* (Appendix 3).

The benthic microalgal communities in Florida Bay are more productive than many other temperate estuaries (Table 6). Under low levels of irradiance (<500 μmol photons m^{-2} s^{-1}), BMA oxygen production in Florida Bay is comparable to that of other shallow temperate estuaries. Low attenuation of light by the water column in Florida Bay means that the benthic communities receive incident irradiances much greater than temperate systems of similar depth. Typical daily irradiance received by the benthos in temperate estuaries ranges from 50 to 600 μmol photons m^{-2} s^{-1} (i.e. Sundback et al. 2000, Dalsgaard 2003), where as the benthos in Florida Bay regularly receive irradiances greater than 1000 μmol photons m^{-2} s^{-1}.

Furthermore, BMA primary production directly alters nitrogen cycling through N-assimilation to support production. In Florida Bay, this nutrient removal may be an important driver of nutrient limitations in the water column. Long-term trends of high TN:TP and DIN:SRP in the water column (Boyer et al. 1999), seagrass, phytoplankton

		Hourly Production (mg C m^{-2} h^{-1})		Chl-*a* (mg chl m^{-2})	Source
Temperate Systems					
Chukchi Sea, Alaska, USA [a]	71º 16'N	<5 - 57	^{14}C		Matheke & Horner 1974
Ragardsvik, Sweden [bcd]	58º 12'N	<1 - 5	O_2	60 - 130	Sundback et al. 2003
Gulmar Fjord, Sweden [bde]	58º 22'N	2 - 20	O_2	90 - 100	Sundback et al. 2004
Yithan Estuary, Scotland [a]	57º 20'N	2 - 23	^{14}C		Leach 1970
Lovns Broad, Denmark [bcd]	56º 37'N	10 - 180	O_2	50 - 275	Dalsgaard 2003
Kertinge Nor, Denmark [bcd]	55º N	<1 - 7	O_2		Rysgaard et al. 1995
Ems-Dollard Estuary, Netherlands [a]	53º 30'N	<10 - 115	^{14}C	10 - 420	Colijn & de Jonge 1984
Colne River Estuary, England [bcd]	51º 45'N	1 - 78	O_2		Dong et al. 2000
River Lynher, England [a]	51º 15'N	5 - 115	^{14}C		Joint 1978
Netarts Bay, Oregon, USA [a]	45º 25'N	<5 - 88	O_2		Davis & McIntire 1983
Golfe de Fos, France [a]	43º 23'N	1 - 21	O_2		Plante-Cuny & Bodoy 1987
Ria de Arosa, Spain [a]	42º 24'N	3 - 44	^{14}C		Varela & Penas 1985
Sippewissett Marsh, Massachuesetts, USA [a]	41º 33'N	<5 - 85	^{14}C		Van Raalte et al. 1976
Block Island Sound, Rhode Island, USA [a]	41º 25'N	<5 - 105	^{14}C		Marshall et al. 1971
Block Island Sound, Rhode Island, USA [a]	41º 25'N	0 - 164	^{14}C		Marshall et al. 1972
Long Island Sound, Connecticut, USA [a]	41º 17'N	4 - 33	O_2		Baille 1986
Hog Island Bay, Virginia, USA [bc]	37º 30'N	5 - 10	DIC	10 - 85	McGlathery et al. 2001
Chesapeake Bay, Virginia, USA [a]	37º 17'N	<2 - 68	O_2	5 - 65	Rizzo & Wetzel 1985
Mugu Lagoon, California, USA [a]	34º 06'N	8 - 36	O_2		Shaffer & Onuf 1983
Bolsa Bay, California, USA [a]	33º 47'N	5 - 125	^{14}C		Riznyk et al. 1978
North Inlet Estuary, South Carolina, USA [a]	33º 20'N	19 - 180	O_2		Pinkney & Zingmark 1993a
Graveline Bay Mississippi, USA [a]	30º 24'N	<5 - 56	^{14}C		Sullivan & Moncrieff 1988

		Hourly Production (mg C m^{-2} h^{-1})		Chl-*a* (mg chl m^{-2})	Source
Sub-tropical andTropical Systems					
Galveston Bay, Texas, USA[bcd]	29º 23'N	<0 - 7	O_2		An & Joy 2001
San Antonio Bay, Texas, USA [a]	29º 19'N	<1 - 11	^{14}C	2 - 36	MacIntyre & Cullen 1996
Sydney Lagoons, Australia[bc]	35º 55'S	0 - 10	O_2		Eyre & Ferguson 2003
Brunswick and Sandon Rivers, New South Wales, Australia [cd]	28º 35'S 29º 41'S	12 - 46	O_2	3 - 45	Ferguson et al. 2003
Sunset Cove, Florida, USA [cd]	25º 05'N				Present Study
January 2004		25 – 110	O_2	24 – 104	
March 2004		64 – 121	O_2	33 – 110	
June 2004		13 – 150	O_2	46 – 108	
July 2004		26 – 64	O_2	25 – 78	

[a] Adapted from MacInytre et al. 1996, PQ=1
[b] Estimated from a figure
[c] GPP estimate from NPP and CR (light and dark oxygen fluxes, respectively)
[d] PQ=1.2
[e] Range of values presented from stations at ≤5m depth

Table 6. Range of semi-annual to annual variability in BMA gross primary production (presented at carbon uptake) and biomass (where available) in temperate and subtropical-tropical estuaries and lagoons. The original method of quantifying BMA production is indicated to the right of the hourly production rates:^{14}C uptake (^{14}C), DIC uptake (DIC), or oxygen evolution (O_2).

and epiphyte tissue (Zieman et al. 1989, Forqurean et al. 1992, Fourqurean et al. 1993, Fourqurean & Zieman 2002, Armitage et al. 2005) show P-limitation in northeastern Florida Bay. However, relative P availability increases in the western portions of Florida Bay due to exchange with the Gulf of Mexico (Zieman et al. 1989, Fourqurean & Zieman 2002) and there is evidence of N-limitation in some regions (Fourqurean & Zieman 2002). The observed rates of BMA production in the present study occur despite P-limitation in the eastern areas of Florida Bay. The large amount of N required to support the observed rates of BMA primary production (1.5-14.4 mmol N m^{-2} d^{-1}) may help induce N-limitation in some areas of Florida Bay, especially those with relatively higher P availabiltiy.

If the N-demand to support the observed rates of primary production is fully realized, BMA assimilation of the diffusive NH_4^+ flux would account for 8-58% of the BMA N-demand under low light conditions and less than 10% of the total BMA N-demand during high light conditions (Table 5). Nitrogen fixation in Florida Bay ranges from 7.13 - 478 μmol N m^{-2} d^{-1} (Nagel 2004), and would only meet a small fraction of the total BMA nitrogen demand. Furthermore, the estimated N-demand during all light conditions also exceeds the observed NH_4^+ flux and the net flux to the sediment surface (Diffusive + |Observed|). Fick's First law is a reasonable approximation for diffusive fluxes in coarse sediments but may underestimate the diffusive flux in the presence of bioirrigation and bioturbation (Lavery et al. 2001). Additional fluxes of nitrogen from bioirrgation or bioturbation could provide additional nutrients to support

BMA production. If these additional fluxes do not exceed the BMA N-demand, they would not have been observed in the batch core incubations.

Zones of BMA production and sulfide interactions

Oxygen dynamics in surface sediment are controlled by benthic microalgae (e.g. Rysgaard et al. 1995) and rooted macrophytes (Lee & Dunton 2000) on a diel scale, but seagrass and BMA have very different depth zones which they affect. While the seagrass rhizosphere is 5-10 cm below the sediment surface, oxygen production by benthic microalgae is limited to the top centimeter of sediment and the maximum oxygen penetration depth varies. BMA production causes diurnal variation in sediment oxygen concentration, particularly in the surface 1.5 mm of sediment (Rysgaard et al. 2000), and can increase sediment O_2 penetration (Revsbech et al. 1983). When sediments from Florida Bay were incubated under artificial light, porewater O_2 concentrations increased but there was little diurnal variation in the zones of maximum oxygen production. In dark and light incubations, the zones of maximum O_2 consumption and production overlapped between 0.7 and 1.7 mm of sediment depth. The overlap of these zones suggests that mobile BMA are constrained to a 2 mm zone just below the sediment surface. The observed respiration at the surface during light incubations in this study (Fig.8) suggests either inaccurate determination of the sediment-water interface (Glud et al. 1992) or stimulated production by heterotrophic bacteria on the surface sediment (Jorgensen & Revsbech 1985). Detritus from adjacent seagrass beds as well as excess production by the BMA (Middelburg et al. 2000) may support a heterotrophic surface community. Community respiration consumes oxygen during dark periods and diffusion

from oxygenated bottom waters is important to maintain a veneer of aerobic sediments. However, when comparing the penetration depth of compilation profiles, the oxygen penetration depth increased by almost 2mm from low to high irradiances and ~4 mm from dark to high irradiance indicating a spatial heterogeneity in the oxygen penetration depth between replicate cores. This spatial heterogeneity may be important to sediment oxygen dynamics the BMA sediment patch scale.

The maximum depth of the oxygen penetration in sediment porewater doubled between dark and high irradiance (1000μmol photons m^{-2} s^{-1}) periods, from 4 mm to 8 mm. The dynamic zone of the oxic-anoxic boundary in the surface sediments has strong implications for nutrient cycling on a diurnal scale. The increased oxic zone during periods of illumination can stimulate nitrification (Risgaard-Petersen et al. 1994, Rysgaard et al. 1995, An & Joye 2001), provided ample substrate diffuses from deeper sediments. However, within this dynamic zone of the oxic-anoxic boundary, sulfide diffuses upward from deeper sediments when oxygen production ceases (Nelson et al. 1986) and can inhibit nitrification (Joye & Hollibaugh 1995). Joye and Hollibaugh (1995) found that nitrification remains inhibited for up to 24 hours after a brief exposure to hydrogen sulfide. The presence of H_2S was observed as shallow as 5 mm sediment depth in Florida Bay, and may play an important role in preventing nitrogen removal through coupled nitrification-denitrification. In this study, nitrification rates were not quantified and the degree to which sulfide inhibits nitrification could not be fully determined. Furthermore, denitrification could not be used as an indicator of nitrification inhibition because it was not be accurately measured during periods of production.

Nutrient fluxes and denitrificaiton

Benthic microalgae act as filters to control the release of inorganic nitrogen from sediment to the water column (e.g. Krom 1991, Anderson et al. 2003, Sundback et al. 2003) . Although the porewater in Florida Bay is highly enriched with respect to NH_4^+, there is very little NH_4^+ efflux to the water column, suggesting several mechanisms of internal N-recycling in the surface sediments. N-assimilation at the sediment-water interface can consume mineralization products and high rates of mineralization are not always reflected as an efflux to the water column (Rysgaard et al. 1996, Sundback et al. 2000, Anderson et al. 2003). The N-demand to support the observed rates of oxygen production is sufficient to prevent the release of NH_4^+ to the water column (Table 5). The observation of low inorganic N fluxes to the water column further supports BMA assimilation of remineralized nutrients as a key mechanism to internal N-cycling.

Sediments can act as either a nutrient source or sink depending on many biogeochemical parameters of an estuary. Benthic microalgae are also in competition with the bacterial community for inorganic nitrogen. Coupled nitrification-denitrificaion (Rysgaard et al. 1995), nitrate reduction by sulfur oxidizing bacteria (Revsbech et al. 1983, Lee & Dunton 2000), dissimilatory nitrate reduction to ammonium (DNRA) (Gardner et al. 2005), and assimilation by BMA (e.g. Thornton et al. 2002) all compete for available nitrate. Although there is the potential for such competition to reduce BMA productivity through N-limitation, this study suggest that BMA N-assimilation and oxygen production limits microbial N-cycling processes.

Conclusion

Benthic microalgae in Florida Bay are a highly productive component of the benthic community in both seagrass and macrophyte-free habitats. Production at irradiances less than 500 μmol photons m^{-2} s^{-1} is comparable to that observed in temperate systems. When irradiances exceed 500 μmol photons m^{-2} s^{-1} BMA in Florida Bay are substantially more productive than their temperate counterparts, despite the potential for nutrient limitation. Compared to temperate systems, Florida Bay BMA fulfills similar ecological functions by acting like a filter at the sediment-water interface. N-assimilation to support BMA production reduces the release of NH_4^+ from the sediments to the water column, and suggests closed nutrient cycling within the surface centimeter of sediments and BMA. Oxygen production by the BMA deepens the oxic-anoxic boundary in the surface sediments with strong implications for sulfide dynamics. As a result, nitrification and coupled nitrification-denitrification may be inhibited there by reducing nitrogen removal from the sediments. Further competition between bacteria and BMA may also be import in maintaining N-limiting conditions in some areas of Florida Bay. Before nutrient cycling rates can be extrapolated to an ecosystem scale, estimates of mineralization, nitrification and dissimilarity nitrate reduction in Florida Bay are needed.

Appendices

Appendix 1. Bay-wide BMA production and nutrient flux rates

The bay-wide survey of BMA biomass, production and nutrient fluxes was conducted in June 2003. Three replicate cores were collected in each habitat type at each site. The observed fluxes of oxygen, ammonium and nitrogen are presented for each individual core.

Incubation treatment **Habitat type and site**		**BMA Biomass** (mg chl-*a* m^{-2})	**O_2 Flux** (µmol O_2 m^{-2} h^{-1})	**NH_4^+ Flux** (µmol NH_4^+ m^{-2} h^{-1})	**N_2-N Flux** (µmol N_2-N m^{-2} h^{-1})
Dark Incubated:					
Seagrass-free patches:					
Barnes Key Basin	1	34.4	-3976.50	6.23	-9.26
	2	65.0	-5694.41	1.38	-23.64
	3	28.0	-7503.84	88.90	198.06
Rabbit Key Basin	1	10.4	-3949.60	153.62	-256.33
	2	56.2	-3216.24	-18.20	-88.75
	3	14.2	-2457.68	-4.61	6.77
Rankin Bight	1	8.1	-2529.49	19.30	187.08
	2	40.2	-2113.24	-41.87	8.18
	3	35.4	-2478.29	-5.94	-234.30
Sunset Cove	1	21.5	-3237.23	50.11	-56.89
	2	31.1	-5261.32	69.13	26.83
	3	17.2	-6515.47	254.81	34.88
Within seagrass beds:					
Barnes Key Basin	1	9.6	-6193.58	149.05	27.97
	2	4.9	-3819.01	159.33	8.52
	3	3.3	-5016.36	37.27	18.11
Rabbit Key Basin	1	8.3	-2432.96	74.78	25.73
	2	9.2	-1630.63	9.48	57.76
	3	7.8	-1848.74	-19.78	33.94
Rankin Bight	1	6.6	-3370.56	154.99	-198.95
	2	8.4	-1474.37	13.52	25.03
	3	5.5	-2019.00	27.74	-166.43

Incubation treatment Habitat type and site		BMA Biomass (mg chl-*a* m^{-2})	O_2 Flux (μmol O_2 m^{-2} h^{-1})	NH_4^+ Flux (μmol NH_4^+ m^{-2} h^{-1})	N_2-N Flux (μmol N_2-N m^{-2} h^{-1})
Dark Incubated:					
Within seagrass beds:					
Sunset Cove	1	11.1	-1435.98	-38.59	46.12
	2	12.6	-3092.57	67.87	53.57
	3	6.3	-1260.14	-16.19	224.76
Light Incubated:					
Seagrass-free patches:					
Barnes Key Basin	1	34.4	9243.09	-12.21	
	2	28.0	8995.58	-55.71	
	3	65.0	6252.53	-21.16	
Rabbit Key Basin	1	10.4	1204.71	-66.42	
	2	14.2	4227.91	-73.37	
	3	56.2	8704.33	-32.87	
Rankin Bight	1	8.1	1201.21	-37.99	
	2	35.4	10223.23	-33.80	
	3	40.2	4679.09	-16.64	
Sunset Cove	1	21.5	6700.44	-8.05	
	2	17.2	-1496.81	116.39	
	3	31.1	8155.28	42.84	
Within seagrass beds:					
Barnes Key Basin	1	9.6	2180.77	-152.11	
	2	3.3	2135.00	-45.41	
	3	4.9	1419.28	-72.16	
Rabbit Key Basin	1	8.3	-245.94	-14.64	
	2	7.8	732.92	-51.60	
	3	9.2	-367.98	-35.10	
Rankin Bight	1	6.6	873.62	-9.63	
	2	5.5	320.97	-33.65	
	3	8.4	2115.58	-54.09	
Sunset Cove	1	11.1	-1053.83	33.87	
	2	6.3	-1281.01	46.76	
	3	12.6	1844.24	121.85	

Appendix 2. Bay-wide porewater nutrient profiles

Porewater nutrient profiles were collected in June 2003 from within seagrass-free sediment patches and from within seagrass beds at four sites in Florida Bay. The values presented here represent the mean of analytical reps taken from one or two cores collected within each habitat type.

	Depth Interval (cm)	H_2S (μM)	NH_4^+ (μM)	SRP (μM)
Within a seagrass-free sediment patch				
Barnes	0.0-0.5	398.97	58.30	--
	0.5-1.0	1266.79	149.19	1.37
	1.0-1.5	1793.33	353.67	1.63
	1.5-2.0	2031.41	562.37	1.73
	2-3	2077.73	1171.63	1.85
	3-4	1892.46	471.49	1.54
	4-7	1963.97	1631.94	2.23
	7-10	1940.41	2010.62	2.59
Rabbit	0.0-0.5	352.65	134.04	--
	0.5-1.0	890.57	245.12	0.76
	1.0-1.5	1111.59	309.07	0.85
	1.5-2.0	1332.61	327.59	1.33
	2-3	1633.26	399.96	1.01
	3-4	1916.03	443.72	1.35
	4-7	1992.41	686.07	1.77
	7-10	1855.90	946.95	2.93
Rankin	0.0-0.5	266.52	--	--
	0.5-1.0	156.01	49.89	0.27
	1.0-1.5	307.15	134.04	0.39
	1.5-2.0	388.41	219.87	0.46
	2-3	983.20	302.34	0.83
	3-4	957.20	374.71	0.83
	4-7	1301.73	479.06	0.94
	7-10	1254.60	532.92	0.87
Sunset	0.0-0.5	29.25	28.01	--
	0.5-1.0	22.75	38.11	0.22
	1.0-1.5	24.38	41.47	0.26
	1.5-2.0	26.00	57.46	0.21
	2-3	34.94	59.98	0.23
	3-4	49.57	68.40	0.24
	4-7	133.26	84.39	0.28
	7-10	86.94	69.24	0.24

	Depth Interval (cm)	H_2S (μM)	NH_4^+ (μM)	SRP (μM)
Within a seagrass-free sediment patch				
Mean of all sites	0.0-0.5	289.27	54.09	--
	0.5-1.0	604.28	111.60	0.70
	1.0-1.5	842.36	205.57	0.84
	1.5-2.0	972.64	297.85	0.95
	2-3	1114.57	444.28	1.04
	3-4	1187.97	549.75	1.06
	4-7	1248.10	766.30	1.29
	7-10	1194.20	939.93	1.58
Within a seagrass bed				
Barnes	0.0-0.5	101.57	37.26	--
	0.5-1.0	129.20	46.52	0.28
	1.0-1.5	182.01	59.14	0.36
	1.5-2.0	182.83	59.98	0.35
	2-3	319.34	70.92	0.47
	3-4	422.53	80.18	0.46
	4-7	654.93	76.82	0.78
	7-10	945.83	127.31	1.14
Rabbit	0.0-0.5	104.01	43.15	--
	0.5-1.0	705.31	108.79	0.71
	1.0-1.5	848.32	145.82	0.82
	1.5-2.0	1101.84	157.60	0.90
	2-3	988.08	147.50	0.84
	3-4	968.58	122.26	0.73
	4-7	1101.84	102.06	1.61
	7-10	1378.11	95.33	2.02
Rankin	0.0-0.5	8.13	66.72	--
	0.5-1.0	55.25	115.53	0.51
	1.0-1.5	65.01	108.79	0.28
	1.5-2.0	60.13	120.57	0.32
	2-3	266.52	105.43	0.38
	3-4	404.66	157.60	0.46
	4-7	466.41	405.01	
	7-10	581.80	251.85	0.72

	Depth Interval (cm)	H_2S (μM)	NH_4^+ (μM)	SRP (μM)
Within a seagrass bed				
Sunset	0.0-0.5	19.50	13.70	--
	0.5-1.0	29.25	23.80	0.38
	1.0-1.5	63.38	38.11	0.28
	1.5-2.0	87.76	48.20	0.77
	2-3	165.76	57.46	0.30
	3-4	264.90	68.40	0.41
	4-7	417.66	110.48	0.59
	7-10	543.61	137.40	0.63
Mean of all sites	0.0-0.5	59.05	35.30	--
	0.5-1.0	179.58	60.83	0.42
	1.0-1.5	234.02	74.85	0.40
	1.5-2.0	283.86	82.43	0.58
	2-3	370.80	84.95	0.46
	3-4	458.02	96.17	0.49
	4-7	611.70	160.97	0.89
	7-10	798.59	149.86	1.03

Appendix 3. Sunset Cove production and nutrient flux rates

Experimental data from the annual survey of Sunset Cove are presented in this appendix. Six replicate cores were collected from a persistent seagrass-free sediment patch during January, March, June and August 2004. The first table presents the BMA biomass observed in experimental cores, including cores sacrifices for initial porewater characterization. The second table presents the incubation time, shade treatments, and actual observed irradiance in the experimental chamber are presented in this table. The incubation time is the actual time during which the cores were incubated at the given shade treatment. It is presented in Eastern Standard Time for January and March, and Eastern Daylight Savings Time for June and August. Irradiance was observed inside the incubation chamber with submersible photosynthetic irradiance recording systems (Dataflow systems PTY, Ltd.). During high light periods, the observed irradiance in the incubation chamber was very unlike irradiances observed in other locations in and around Florida Bay. Instances were the experimental irradiance was approximated are noted in the table. Additionally, the observed fluxes of oxygen, ammonium, and nitrogen are normalized to both per unit area and per unit benthic chl-*a* for each replicate core. All fluxes presented here have been corrected for water column activity.

	Core	BMA Biomass (mg chl-*a* m^{-2})
January	Initial 1	52.71
	Initial 2	70.63
	Initial 3	39.29
	1	100.36
	2	103.86
	3	24.51
	4	48.52
	5	56.96
	6	49.31
March	Initial 1	33.34
	Initial 2	43.35
	Initial 3	35.00
	1	95.79
	2	99.47
	3	65.87
	4	42.28
	5	47.17
	6	110.40
June	Initial 1	88.70
	Initial 2	51.54
	Initial 3	108.98
	1	75.86
	2	46.16
	3	50.26
	4	90.62
	5	108.78
	6	51.26
August	Initial 1	29.32
	Initial 2	29.63
	Initial 3	37.69
	1	30.40
	2	39.11
	3	38.78
	5	33.32
	6	42.67

Incubation Time	Shade Trt.	Observed Light (μmol photons m^{-2} s^{-1})	Rep.	O_2 Flux (μmol O_2 m^{-2} h^{-1})	NH_4^+ Flux (μmol NH_4^+ m^{-2} h^{-1})	N_2-N Flux (μmol N_2-N m^{-2} h^{-1})	O_2 Flux (μmol O_2 mg chl^{-1} h^{-1})	NH_4^+ Flux (μmol NH_4^+ mg chl^{-1} h^{-1})	N_2-N Flux (μmol N_2-N mg chl^{-1} h^{-1})
January 2004									
0710-0820	Dark	0	1	-2861.33	102.00	163.80	-28.51	1.02	1.63
			2	-3454.33	110.12	148.43	-33.26	1.06	1.43
			3	-2785.51	-197.42	112.09	-113.66	-8.06	4.57
			4	-2839.45	34.30	55.57	-58.52	0.71	1.15
			5	-2078.87	18.13	120.25	-36.50	0.32	2.11
0820-0915	Dark	0	1	-3408.62	207.88	349.75	-33.96	2.07	3.49
			2	-2923.01	-16.80	428.01	-28.14	-0.16	4.12
			3	-1307.24	-74.14	388.49	-53.34	-3.03	15.85
			4	-278.99	-26.97	464.05	-5.75	-0.56	9.56
			5	-1637.45	-92.95	496.71	-28.75	-1.63	8.72
0915-1010	2 Screens	53	1	563.17	-120.44	-78.60	5.61	-1.20	-0.78
			2	3530.45	-47.08	65.88	33.99	-0.45	0.63
			3	279.20	0.39	-72.46	11.39	0.02	-2.96
			4	-1059.49	18.90	-87.29	-21.83	0.39	-1.80
			5	-129.39	-4.24	24.76	-2.27	-0.07	0.43
1010-1115	2 Screens	98	1	7626.83	-226.15	17766.56	76.00	-2.25	177.03
			2	11621.67	-60.90	10820.11	111.90	-0.59	104.18
			3	2768.82	-77.26	387.21	112.98	-3.15	15.80
			4	2137.08	-87.84	364.80	44.04	-1.81	7.52
			5	2159.08	-40.76	332.96	37.91	-0.72	5.85

Incubation Time	Shade Trt.	Observed Light (μmol photons m^{-2} s^{-1})	Rep.	O_2 Flux (μmol O_2 m^{-2} h^{-1})	NH_4^+ Flux (μmol NH_4^+ m^{-2} h^{-1})	N_2-N Flux (μmol N_2-N m^{-2} h^{-1})	O_2 Flux (μmol O_2 mg chl^{-1} h^{-1})	NH_4^+ Flux (μmol NH_4^+ mg chl^{-1} h^{-1})	N_2-N Flux (μmol N_2-N mg chl^{-1} h^{-1})
January 2004									
1115-1217	1 Screen	1290	1	8870.90	-33.70	-4349.66	88.39	-0.34	-43.34
			2	11274.98	-17.39	-5538.83	108.56	-0.17	-53.33
			3	2678.79	-59.82	-486.93	109.31	-2.44	-19.87
			4	2647.35	-52.92	-808.81	54.56	-1.09	-16.67
			5	4916.89	-38.50	-454.91	86.32	-0.68	-7.99
1217-1258	1 Screen	1438	1	13075.75	9.76	-6052.69	130.29	0.10	-60.31
			2	5073.98	-92.61	-3003.59	48.85	-0.89	-28.92
			3	2752.52	9.50	-293.58	112.31	0.39	-11.98
			4	11170.14	9.10	-4586.17	230.20	0.19	-94.52
			5	12351.80	22.31	-6989.07	216.85	0.39	-122.70
1258-1344	Ambient	Apx. 2000	1	12180.98	22.20	-4807.00	121.37	0.22	-47.90
			2	17921.76	22.40	-2935.30	172.55	0.22	-28.26
			3	4504.03	-83.78	-3319.06	183.78	-3.42	-135.43
			4	10430.76	-83.17	-3480.76	214.97	-1.71	-71.73
			5	8916.23	-29.96	-2195.49	156.54	-0.53	-38.54
1344-1417	Ambient	Apx. 2000	1	13685.36	-54.82	-6551.43	136.36	-0.55	-65.28
			2	-584.33	-71.23	-6064.79	-5.63	-0.69	-58.39
			3	2252.02	-18.86	118.25	91.89	-0.77	4.83
			4	-9736.08	-89.28	7553.65	-200.65	-1.84	155.67
			5	-94.26	-9.35	1380.16	-1.65	-0.16	24.23

Incubation Time	Shade Trt.	Observed Light (μmol photons m^{-2} s^{-1})	Rep.	O_2 Flux (μmol O_2 m^{-2} h^{-1})	NH_4^+ Flux (μmol NH_4^+ m^{-2} h^{-1})	N_2-N Flux (μmol N_2-N m^{-2} h^{-1})	O_2 Flux (μmol O_2 mg chl^{-1} h^{-1})	NH_4^+ Flux (μmol NH_4^+ mg chl^{-1} h^{-1})	N_2-N Flux (μmol N_2-N mg chl^{-1} h^{-1})
March 2004									
0656-0800	Dark	0	1	-3315.11	-164.45	-254.06	-34.61	-1.72	-2.65
			2	-3434.71	29.62	126.92	-34.53	0.30	1.28
			3	-3673.44	-69.20	124.53	-55.77	-1.05	1.89
			4	-2967.86	-79.08	203.66	-70.20	-1.87	4.82
			5	-1863.83	-22.81	200.89	-39.51	-0.48	4.26
			6	-3179.58	-71.67	190.27	-28.80	-0.65	1.72
0800-0856	Dark	0	1	-2517.22	12.47	1000.17	-26.28	0.13	10.44
			2	-3619.35	46.98	136.89	-36.39	0.47	1.38
			3	-3044.60	11.84	131.78	-46.22	0.18	2.00
			4	-2827.79	-3.84	176.39	-66.89	-0.09	4.17
			5	-2117.16	31.29	34.19	-44.88	0.66	0.72
			6	-2981.33	12.47	88.74	-27.00	0.11	0.80
0856-1000	2 Screens	47	1	6153.48	-77.65	-1148.05	64.24	-0.81	-11.98
			2	2444.66	45.33	-270.01	24.58	0.46	-2.71
			3	1710.97	-47.18	-269.29	25.97	-0.72	-4.09
			4	3361.95	-30.98	-299.33	79.52	-0.73	-7.08
			5	1614.94	-14.51	-244.21	34.23	-0.31	-5.18
			6	5405.47	-49.10	7735.61	48.96	-0.44	70.07
1000-1100	2 Screens	89	1	7807.62	168.22	11192.81	81.50	1.76	116.84
			2	2105.33	-48.45	1033.18	21.17	-0.49	10.39
			3	3024.43	68.38	-431.89	45.92	1.04	-6.56

Incubation Time	Shade Trt.	Observed Light (μmol photons m^{-2} s^{-1})	Rep.	O_2 Flux (μmol O_2 m^{-2} h^{-1})	NH_4^+ Flux (μmol NH_4^+ m^{-2} h^{-1})	N_2-N Flux (μmol N_2-N m^{-2} h^{-1})	O_2 Flux (μmol O_2 mg chl^{-1} h^{-1})	NH_4^+ Flux (μmol NH_4^+ mg chl^{-1} h^{-1})	N_2-N Flux (μmol N_2-N mg chl^{-1} h^{-1})
March 2004									
1000-1100	2 Screens	89	4	4872.60	37.93	-403.45	115.26	0.90	-9.54
			5	1404.55	-43.76	-322.76	29.77	-0.93	-6.84
			6	7084.04	107.32	-2084.53	64.17	0.97	-18.88
1000-1132	1 Screen	659	1	9873.89	-305.02	-3675.37	103.08	-3.18	-38.37
			2	5633.48	-107.38	-1347.77	56.63	-1.08	-13.55
			3	5916.89	-34.37	636.82	89.83	-0.52	9.67
			4	-278.70	-32.17	-1307.46	-6.59	-0.76	-30.93
			5	4283.36	59.51	544.49	90.80	1.26	11.54
			6	10374.19	-219.38	-2652.63	93.97	-1.99	-24.03
1132-1159	1 Screen	829	1	11620.19	-33.10	-3693.22	121.30	-0.35	-38.55
			2	6642.42	-18.13	-3358.88	66.78	-0.18	-33.77
			3	7826.00	-46.76	1813.27	118.81	-0.71	27.53
			4	9170.90	-78.64	11529.50	216.93	-1.86	272.72
			5	3629.02	-1.87	1082.06	76.93	-0.04	22.94
			6	11757.16	34.57	-3137.77	106.49	0.31	-28.42
1229-1300	Ambient	Apx. 2000	1	8858.44	112.32	-2713.24	92.47	1.17	-28.32
			2	6580.09	21.65	10409.21	66.15	0.22	104.65
			3	9565.93	111.19	-2882.08	145.22	1.69	-43.75
			4	9034.40	66.42	367.54	213.70	1.57	8.69
			5	5135.83	114.59	270.58	108.87	2.43	5.74
			6	8391.90	82.85	-1311.34	76.01	0.75	-11.88

Incubation Time	Shade Trt.	Observed Light (μmol photons m^{-2} s^{-1})	Rep.	O_2 Flux (μmol O_2 m^{-2} h^{-1})	NH_4^+ Flux (μmol NH_4^+ m^{-2} h^{-1})	N_2-N Flux (μmol N_2-N m^{-2} h^{-1})	O_2 Flux (μmol O_2 mg chl^{-1} h^{-1})	NH_4^+ Flux (μmol NH_4^+ mg chl^{-1} h^{-1})	N_2-N Flux (μmol N_2-N mg chl^{-1} h^{-1})
March 2004									
1159-1229	Ambient	Apx. 2000	1	13726.69	69.18	-7926.45	143.30	0.72	-82.75
			2	8462.71	-68.44	-3239.67	85.08	-0.69	-32.57
			3	9279.73	-67.27	-5448.82	140.88	-1.02	-82.72
			4	6563.38	-52.63	-8673.13	155.25	-1.24	-205.15
			5	4468.99	-134.61	-3180.43	94.73	-2.85	-67.42
			6	11834.85	-22.17	-5066.99	107.20	-0.20	-45.90
June 2004									
0835-0940	Dark	0	1	-7071.53	-81.37	68.92	-93.21	-1.07	0.91
			2	-4513.59	-53.31	15.58	-97.79	-1.15	0.34
			3	-4102.55	66.22	75.73	-81.63	1.32	1.51
			4	-6948.60	129.80	130.27	-76.68	1.43	1.44
			5	-6147.39	99.07	-18.36	-56.51	0.91	-0.17
			6	-5541.41	81.51	21.12	-108.11	1.59	0.41
0940-1040	Dark	0	1	-4690.14	93.56	-156.66	-61.82	1.23	-2.06
			2	-2137.96	42.56	-18.09	-46.32	0.92	-0.39
			3	-2798.00	-36.40	3.41	-55.67	-0.72	0.07
			4	-3780.73	96.62	54.54	-41.72	1.07	0.60
			5	-3629.48	-8.87	23.96	-33.36	-0.08	0.22
			6	-4091.03	108.08	58.99	-79.82	2.11	1.15
0730-0835	Ambient	63	1	-5720.13	-101.46	-190.75	-75.40	-1.34	-2.51
			2	-2374.93	96.97		-51.45	2.10	
			3	-774.32	-99.09	-17.51	-15.41	-1.97	-0.35
			4	-6039.87	-28.44	-229.69	-66.65	-0.31	-2.53

Incubation Time	Shade Trt.	Observed Light (μmol photons m^{-2} s^{-1})	Rep.	O_2 Flux (μmol O_2 m^{-2} h^{-1})	NH_4^+ Flux (μmol NH_4^+ m^{-2} h^{-1})	N_2-N Flux (μmol N_2-N m^{-2} h^{-1})	O_2 Flux (μmol O_2 mg chl^{-1} h^{-1})	NH_4^+ Flux (μmol NH_4^+ mg chl^{-1} h^{-1})	N_2-N Flux (μmol N_2-N mg chl^{-1} h^{-1})
June 2004									
0730-0835	Ambient	63	5	-3258.13	-36.56	-17.42	-29.95	-0.34	-0.16
			6	-2154.69	-29.10	450.58	-42.04	-0.57	8.79
1040-1135	2 Screens	616	1	3375.83	-48.95	-10462.44	44.50	-0.65	-137.91
			2	1398.01	163.36	847.54	30.29	3.54	18.36
			3	6081.11	-19.25	-0.14	120.99	-0.38	0.00
			4	2127.14	62.26	10.55	23.47	0.69	0.12
			5	5869.07	5.90	-8878.39	53.95	0.05	-81.62
			6	167.15	27.28	13.67	3.26	0.53	0.27
1135-1235	2 Screens	1079	1	8560.92	-22.64	146.33	112.85	-0.30	1.93
			2	4025.49	-197.41	-525.88	87.21	-4.28	-11.39
			3	10262.26	-16.62	14225.12	204.18	-0.33	283.03
			4	10414.95	-226.16	260.14	114.93	-2.50	2.87
			5	9327.82	100.67	148.15	85.75	0.93	1.36
			6	1148.74	176.42	215.26	22.41	3.44	4.20
1325-1405	1 Screen	1427	1	12066.14	17.63	14561.08	159.05	0.23	191.94
			2	-464.78	-28.45	141.76	-10.07	-0.62	3.07
			3	8662.17	-41.48	-3840.86	172.35	-0.83	-76.42
			4	8246.68	-124.02	14281.27	91.00	-1.37	157.59
			5	13676.74	-13.06	-4968.55	125.72	-0.12	-45.67
			6	6623.20	34.90	212.99	129.22	0.68	4.16

Incubation Time	Shade Trt.	Observed Light (μmol photons m^{-2} s^{-1})	Rep.	O_2 Flux (μmol O_2 m^{-2} h^{-1})	NH_4^+ Flux (μmol NH_4^+ m^{-2} h^{-1})	N_2-N Flux (μmol N_2-N m^{-2} h^{-1})	O_2 Flux (μmol O_2 mg chl^{-1} h^{-1})	NH_4^+ Flux (μmol NH_4^+ mg chl^{-1} h^{-1})	N_2-N Flux (μmol N_2-N mg chl^{-1} h^{-1})
June 2004									
1235-1325	1 Screen	1758	1	14540.93	-27.60	77.09	191.67	-0.36	1.02
			2	4617.02	-27.77	107.29	100.03	-0.60	2.32
			3	12359.36	21.49	-4851.26	245.91	0.43	-96.52
			4	9733.23	8.81	-238.68	107.40	0.10	-2.63
			5	14471.16	-140.30	11582.29	133.03	-1.29	106.47
			6	6142.36	-311.03	108.41	119.84	-6.07	2.12
1446-1526	Ambient	2129	1	11795.40	18.24	-4026.15	155.48	0.24	-53.07
			2	812.10	18.19	7.49	17.59	0.39	0.16
			3	2485.71	-37.48	-469.32	49.46	-0.75	-9.34
			4	13308.34	-45.68	-4859.12	146.85	-0.50	-53.62
			5	10336.74	2.47	-2670.80	95.02	0.02	-24.55
			6	5639.73	-62.33	129.06	110.03	-1.22	2.52
1405-1446	Ambient	2740	1	16892.60	-40.94	-5822.90	222.67	-0.54	-76.76
			2	2704.05	-71.19	92.18	58.58	-1.54	2.00
			3	10606.88	74.39	-3743.05	211.04	1.48	-74.47
			4	10889.32	3.46	-2636.46	120.16	0.04	-29.09
			5	8142.14	-87.32	-3256.25	74.85	-0.80	-29.93
			6	8684.85	3.33	68.87	169.44	0.06	1.34
August 2004									
0755-0855	Dark	0	1	-2708.47	370.72	-130.45	-89.10	12.20	-4.29
			2	-4694.88	376.11	-25.52	-120.05	9.62	-0.65
			3	-3235.31	362.85	484.91	-83.43	9.36	12.50
			4	-2406.85	174.16	57.93			

Incubation Time	Shade Trt.	Observed Light (μmol photons m^{-2} s^{-1})	Rep.	O_2 Flux (μmol O_2 m^{-2} h^{-1})	NH_4^+ Flux (μmol NH_4^+ m^{-2} h^{-1})	N_2-N Flux (μmol N_2-N m^{-2} h^{-1})	O_2 Flux (μmol O_2 mg chl^{-1} h^{-1})	NH_4^+ Flux (μmol NH_4^+ mg chl^{-1} h^{-1})	N_2-N Flux (μmol N_2-N mg chl^{-1} h^{-1})
August 2004									
0755-0855	Dark	0	5	-2885.58	-463.11	34.45	-86.61	-13.90	1.03
			6	-3561.41	394.89	43.57	-83.47	9.25	1.02
0855-0955	Dark	1	1	-2589.24	82.45	52.68	-85.18	2.71	1.73
			2	-4361.40	-23.33	75.97	-111.52	-0.60	1.94
			3	-2443.99	-134.50	1515.52	-63.03	-3.47	39.08
			4	-2437.92	-249.89	82.99			
			5	-3134.06	8.27	-261.16	-94.07	0.25	-7.84
			6	-4246.03	-309.25	123.18	-99.51	-7.25	2.89
0955-1055	2 Screens	59	1	525.38	36.46	-287.44	17.28	1.20	-9.46
			2	-2472.52	176.81	-133.03	-63.22	4.52	-3.40
			3	-1209.04	134.55	-1202.18	-31.18	3.47	-31.00
			4	660.90	-7.23	-107.37			
			5	-149.54	-189.91	258.32	-4.49	-5.70	7.75
			6	-719.18	215.11	-345.13	-16.86	5.04	-8.09
1055-1155	2 Screens	76	1	4699.06		-112.47	154.58		-3.70
			2	110.31	49.51	-62.28	2.82	1.27	-1.59
			3	311.71	-1.18	-29.42	8.04	-0.03	-0.76
			4	3565.52	-64.69	9.68			
			5	3631.63	-50.44	250.77	109.01	-1.51	7.53
			6	1193.21		-102.48	27.96		-2.40
1155-1240	1 Screen	880	1	2642.09	-116.00	-157.20	86.92	-3.82	-5.17
			2	2468.58	26.77	111.76	63.12	0.68	2.86

Incubation Time	Shade Trt.	Observed Light (μmol photons m^{-2} s^{-1})	Rep.	O_2 Flux (μmol O_2 m^{-2} h^{-1})	NH_4^+ Flux (μmol NH_4^+ m^{-2} h^{-1})	N_2-N Flux (μmol N_2-N m^{-2} h^{-1})	O_2 Flux (μmol O_2 mg chl^{-1} h^{-1})	NH_4^+ Flux (μmol NH_4^+ mg chl^{-1} h^{-1})	N_2-N Flux (μmol N_2-N mg chl^{-1} h^{-1})
August 2004									
1155-1240	1 Screen	880	3	1486.86	-142.61	-120.23	38.34	-3.68	-3.10
			4	2524.48	-2.81	-31.28			
			5	1891.89	-17.02	-78.85	56.79	-0.51	-2.37
			6	1928.42		56.01	45.20		1.31
1240-1325	1 Screen	919	1	3542.81	27.73	125.93	116.55	0.91	4.14
			2	1784.55	-1.27	32.96	45.63	-0.03	0.84
			3	2554.10	97.14	-121.30	65.86	2.50	-3.13
			4	3597.50	-0.11	42.92			
			5	3365.54		-66.35	101.02		-1.99
			6	2509.35	109.78	630.85	58.81	2.57	14.78
1325-1355	Ambient	1664	1	3654.15	240.75	61.13	120.21	7.92	2.01
			2	4638.58	109.87	474.58	118.61	2.81	12.14
			3	3410.23	204.31	273.49	87.94	5.27	7.05
			4	3980.92	310.65	348.98			
			5	1760.62		305.84	52.85		9.18
			6	3714.86	327.75	-135.10	87.06	7.68	-3.17
1355-1435	Ambient	1917	1	3408.92	-318.10	-155.76	112.14	-10.46	-5.12
			2	3650.03	-330.09	-189.24	93.33	-8.44	-4.84
			3	2498.55	-304.99	-119.44	64.43	-7.87	-3.08
			4	4358.09	-427.13	-556.62			
			5	1660.32		-184.76	49.84		-5.55
			6	2231.20	-369.13	-392.92	52.29	-8.65	-9.21

Appendix 4. Sunset Cove porewater nutrient profiles and sediment characteristics

Porewater nutrient profiles were collected from Sunset Cove 2004 within seagrass-free sediment patch. The values presented here represent the mean of analytical replicates taken individual cores. Initial porewater characteristics were sample on three cores following the acclimation period but immediately prior to the incubation periods. Final porewater characteristics were measured on three, randomly selected, experimental sediment cores following the incubation period. There was no significant difference between initial and final porewater characteristics and the cores were ultimately pooled for a sample size of 6 cores for each month. Bulk density and porosity were measured on different cores than final porewater characteristics.

	Depth Interval (cm)	**H_2S** (μM)	**NH_4^+** (μM)	**SRP** (μM)	**Bulk Density** (gdw ml^{-1})	**Porosity** (ml/ml)
January 2004						
Initial 1	0.0-0.5	13.00	19.90			
	0.5-1.0	50.38	57.23	0.418		
	1.0-1.5	108.88	140.51	0.260		
	1.5-2.0	56.88	159.18	0.438		
	2-3	214.52	209.43	0.616		
	3-4	451.79	265.42	0.655		
	4-7	1062.84	327.16	1.387		
	7-10	476.16	433.41	1.604		
Initial 2	0.0-0.5	24.38	12.73	0.459		
	0.5-1.0	19.50	32.83			
	1.0-1.5		45.75	0.418		
	1.5-2.0	234.02	54.36	0.438		
	2-3	53.63	60.11	0.141		
	3-4	19.50	60.11			
	4-7	40.63	62.98	0.319		
	7-10	53.63	67.29	0.695		
Initial 3	0.0-0.5	120.26	32.83			
	0.5-1.0	183.64	71.59	0.392		
	1.0-1.5	160.89	94.56	0.141		
	1.5-2.0	60.13	98.87	0.912		
	2-3	199.89	121.84	0.240		
	3-4	303.90	157.74	0.912		
	4-7	845.07	297.01	0.299		
	7-10	672.80	219.48	1.743		

	Depth Interval (cm)	H_2S (μM)	NH_4^+ (μM)	SRP (μM)	Bulk Density (gdw ml^{-1})	Porosity (ml/ml)
January 2004						
Final 1	0.0-0.5	81.26	74.46	0.514	0.10	
	0.5-1.0	141.39	114.67	0.432	0.12	
	1.0-1.5	253.52	139.07	0.446	0.14	
	1.5-2.0	360.78	166.35	0.459	0.19	
	2-3	503.79	190.76	0.622	0.26	
	3-4	583.42		0.432	0.33	
	4-7	687.43	219.48	0.473	0.40	
	7-10	536.29	192.20	0.446	0.38	
Final 2	0.0-0.5	34.13	22.78	0.798		
	0.5-1.0	56.88	54.36	0.432	0.13	
	1.0-1.5	50.38	68.72	0.446	0.18	
	1.5-2.0	42.25	78.77	0.446	0.23	
	2-3	107.26	93.13	0.459	0.24	
	3-4	198.27	130.46	0.405	0.26	
	4-7	533.04	183.58	0.378	0.35	
	7-10	516.79	189.33	0.432	0.39	
Final 3	0.0-0.5	19.50	17.03	0.446	0.11	
	0.5-1.0	45.50	41.44	0.419	0.12	
	1.0-1.5	78.01	71.59	0.042	0.12	
	1.5-2.0	84.51	84.51	0.299	0.14	
	2-3	172.26	100.31	0.339	0.20	
	3-4	308.77	137.64	0.200	0.31	
	4-7	589.92	180.71	0.042	0.40	
	7-10	466.41	203.68	0.319	0.45	
March 2004						
Initial 1	0.0-0.5	30.88	72.44			
	0.5-1.0	45.50	72.44			
	1.0-1.5	63.38	118.55			
	1.5-2.0	60.13	114.36			
	2-3	108.88	135.31			
	3-4	95.88	138.11			
	4-7	269.77	168.85			
	7-10	193.39	175.83			
Initial 2	0.0-0.5	27.63	62.66			
	0.5-1.0	32.50	78.03			
	1.0-1.5	48.75	96.19			
	1.5-2.0	35.75	114.36			
	2-3	86.13	131.12			

	Depth Interval (cm)	H_2S (μM)	NH_4^+ (μM)	SRP (μM)	Bulk Density (gdw ml^{-1})	Porosity (ml/ml)
March 2004						
Initial 2	3-4	131.64	164.65			
	4-7	515.17	237.31			
	7-10	682.55	312.76			
Initial 3	0.0-0.5	47.13	85.01			
	0.5-1.0	55.25	97.59			
	1.0-1.5	65.01	124.14			
	1.5-2.0	66.63	122.74			
	2-3	102.38	142.30			
	3-4	370.53	212.16			
	4-7	568.80	255.47			
	7-10	550.92	249.88			
Final 1	0.0-0.5	34.13	85.01		0.11	
	0.5-1.0	71.51	119.94		0.16	
	1.0-1.5	196.64	189.80		0.25	
	1.5-2.0	292.52	242.90		0.28	
	2-3	809.31	308.57		0.31	
	3-4	767.06	351.88		0.34	
	4-7	1322.86	438.51		0.35	
	7-10	1441.49	518.15		0.35	
Final 2	0.0-0.5	56.88	117.15		0.11	
	0.5-1.0	266.52	206.57		0.15	
	1.0-1.5	308.77	256.87		0.19	
	1.5-2.0	456.66	263.86		0.26	
	2-3	555.79	265.25		0.26	
	3-4	970.20	367.25		0.24	
	4-7	1472.37	520.94		0.32	
	7-10	1677.13	731.92		0.41	
Final 3	0.0-0.5	43.88	66.85		0.12	
	0.5-1.0	42.25	93.40		0.20	
	1.0-1.5	34.13	111.56		0.32	
	1.5-2.0	39.00	107.37		0.35	
	2-3	52.00	110.16		0.38	
	3-4	97.51	154.87		0.43	
	4-7	459.91	242.90		0.41	
	7-10	1035.21	364.45		0.49	

	Depth Interval (cm)	H_2S (μM)	NH_4^+ (μM)	SRP (μM)	Bulk Density (gdw ml^{-1})	Porosity (ml/ml)
June 2004						
Initial 1	0.0-0.5	22.12	7.00	0.460		
	0.5-1.0	55.31	34.35	0.622		
	1.0-1.5	123.51	78.80	0.608		
	1.5-2.0	258.09	124.96	0.581		
	2-3	481.15	152.31	1.495		
	3-4	554.89	160.86	0.568		
	4-7	438.75				
	7-10			0.554		
Initial 2	0.0-0.5	9.22	10.42			
	0.5-1.0	16.59	27.52	0.541		
	1.0-1.5	20.28	34.35			
	1.5-2.0	20.28	41.19	0.554		
	2-3	20.28	46.32	0.554		
	3-4	44.24				
	4-7	304.18	155.73	0.554		
	7-10	654.44	236.08	1.078		
Initial 3	0.0-0.5	44.24	5.29			
	0.5-1.0	68.21	12.13	0.595		
	1.0-1.5	125.36	30.94	0.527		
	1.5-2.0	331.83	87.35	0.917		
	2-3	647.07	142.05	0.796		
	3-4	875.66	181.37	0.917		
	4-7	962.31	234.37	1.629		
	7-10	571.49	261.72			
Final 1	0.0-0.5	25.81	20.68		0.21	0.96
	0.5-1.0	29.50	22.39	0.514	0.33	0.94
	1.0-1.5	22.12	41.19	0.487	0.38	0.95
	1.5-2.0	29.50	51.45		0.35	0.92
	2-3	47.93	54.87	0.514	0.38	0.87
	3-4	51.62	51.45	0.622	0.41	0.85
	4-7	116.14	118.12		0.42	0.82
	7-10				0.42	0.84
Final 2	0.0-0.5	40.56	27.52	0.420	0.16	0.96
	0.5-1.0	103.24	78.80	0.541	0.25	0.91
	1.0-1.5	302.33	142.05	0.554	0.32	0.91
	1.5-2.0	376.07	191.63		0.29	0.89
	2-3	711.59	258.30	0.648	0.49	0.82
	3-4	807.45	271.98		0.54	0.81

	Depth Interval (cm)	H_2S (μM)	NH_4^+ (μM)	SRP (μM)	Bulk Density (gdw ml^{-1})	Porosity (ml/ml)
June 2004						
Final 2	4-7	859.07	295.91	0.756	0.52	0.80
	7-10	671.03	273.69	0.581	0.51	0.78
Final 3	0.0-0.5	25.81	1.87		0.12	0.94
	0.5-1.0	70.05	30.94	0.568	0.18	0.88
	1.0-1.5	103.24	54.87	0.487	0.23	0.87
	1.5-2.0	164.07	94.19	0.514	0.22	0.84
	2-3	368.70	152.31	0.689	0.37	0.85
	3-4	543.83	198.47	0.958	0.46	0.85
	4-7	890.41	278.82	1.912	0.46	0.85
	7-10	801.92	283.94	0.514	0.44	0.82
August 2004						
Initial 1	0.0-0.5	18.44	57.29			
	0.5-1.0	486.68	45.47	0.130		
	1.0-1.5	44.24	73.56	0.101		
	1.5-2.0	40.56	69.12	0.101		
	2-3	42.40	85.39	0.101		
	3-4	95.86	114.96	0.115		
	4-7	270.99	143.05	0.231		
	7-10	381.60	174.10	0.231		
Initial 2	0.0-0.5	22.12	49.90			
	0.5-1.0	23.97	76.51	0.101		
	1.0-1.5	46.09	51.38	0.115		
	1.5-2.0	46.09	61.73	0.159		
	2-3	64.52	63.21	0.101		
	3-4	73.74	82.43	0.115		
	4-7	101.39	86.86	0.115		
	7-10	136.42	135.65	0.259		
Initial 3	0.0-0.5	22.12	54.34			
	0.5-1.0	20.28	36.59	0.043		
	1.0-1.5	22.12	55.81	0.086		
	1.5-2.0	46.09	69.12	0.101		
	2-3	66.37	83.91	0.086		
	3-4	81.11	110.52	0.187		
	4-7	280.21	150.44	1.023		
	7-10	455.34	209.58	0.865		

	Depth Interval (cm)	H_2S (μM)	NH_4^+ (μM)	SRP (μM)	Bulk Density (gdw ml^{-1})	Porosity (ml/ml)
August 2004						
Final 1	0.0-0.5	14.75	80.95		0.16	1.00
	0.5-1.0	27.65	82.43	0.058	0.23	0.97
	1.0-1.5	29.50	79.47	0.101	0.27	0.96
	1.5-2.0	35.03	104.61	0.086	0.33	0.90
	2-3	60.84	106.08	0.101	0.35	0.88
	3-4	95.86	128.26	0.101	0.33	0.89
	4-7	258.09	85.39	0.159	0.37	0.88
	7-10	339.20	159.31	0.418	0.39	0.93
Final 2	0.0-0.5	35.03	67.64		0.26	0.95
	0.5-1.0	40.56	86.86	0.130	0.35	0.92
	1.0-1.5	22.12	86.86	0.130	0.53	0.85
	1.5-2.0	70.05	92.78	0.115	0.56	0.83
	2-3	92.18	112.00	0.115	0.51	0.85
	3-4	108.77	134.18	0.130	0.55	0.85
	4-7	84.80	101.65	0.159	0.55	0.83
	7-10	36.87	103.13	0.144	0.48	0.85
Final 3	0.0-0.5	55.31	123.83		0.15	1.00
	0.5-1.0		197.75	0.115	0.22	0.97
	1.0-1.5	228.59	187.40	0.144	0.25	0.96
	1.5-2.0	293.12	231.76	0.173	0.25	0.93
	2-3	352.11	202.19	0.173	0.31	0.92
	3-4	261.78	157.83	0.245	0.38	0.92
	4-7	447.97	154.88	0.231	0.41	0.91
	7-10	127.20	117.91	0.259	0.28	0.90
Final 4	0.0-0.5				0.24	0.86
	0.5-1.0				0.30	0.93
	1.0-1.5				0.36	0.93
	1.5-2.0				0.35	0.93
	2-3				0.36	0.92
	3-4				0.39	0.89
	4-7				0.43	0.89
	7-10				0.33	0.81
Final 5	0.0-0.5				0.17	0.99
	0.5-1.0				0.24	0.96
	1.0-1.5				0.30	0.94
	1.5-2.0				0.37	0.91
	2-3				0.37	0.90
	3-4				0.41	0.96

	Depth Interval (cm)	H_2S (μM)	NH_4^+ (μM)	SRP (μM)	Bulk Density (gdw ml^{-1})	Porosity (ml/ml)
August 2004						
Final 5	4-7				0.36	0.88
	7-10				0.30	0.92
Final 6	0.0-0.5				0.15	1.00
	0.5-1.0				0.20	0.99
	1.0-1.5				0.23	0.87
	1.5-2.0				0.26	0.95
	2-3				0.38	0.89
	3-4				0.34	0.91
	4-7				0.34	0.91
	7-10				0.35	0.88

Appendix 5. Microelectrode profiles

Porewater oxygen concentration profiles measured with a Clarke type microelectrode (OX-25 fast , Uniscence, Denmark). Cores were collected from Sunset Cove, Florida Bay and returned to Cambridge, Maryland within 48-hours of collection. Incubation and profiling was conducted under artificial lighting in an environmental growth chamber. Each core was profiled in two or three randomly chosen location at each light level. The measured oxygen concentration profile is presented for each core, with replicate locations, at each light level.

Dark porewater O_2 profiles:

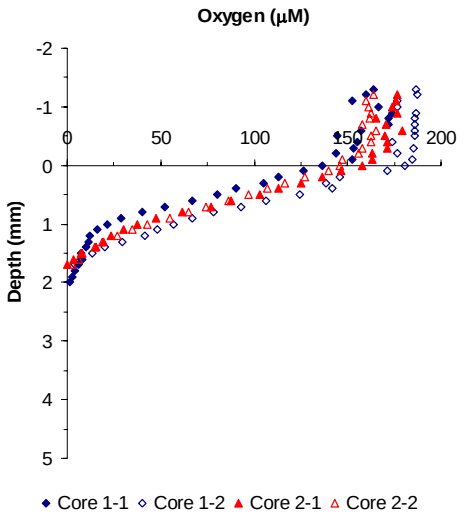

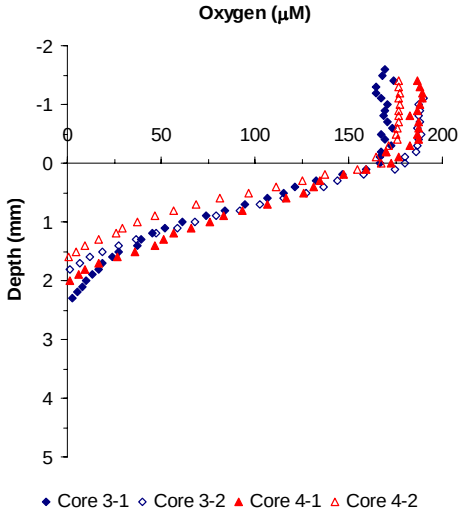

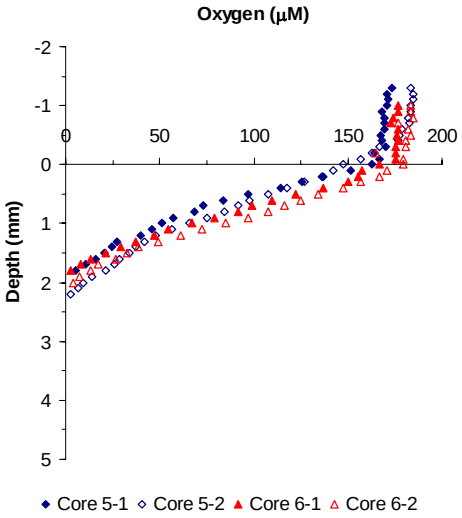

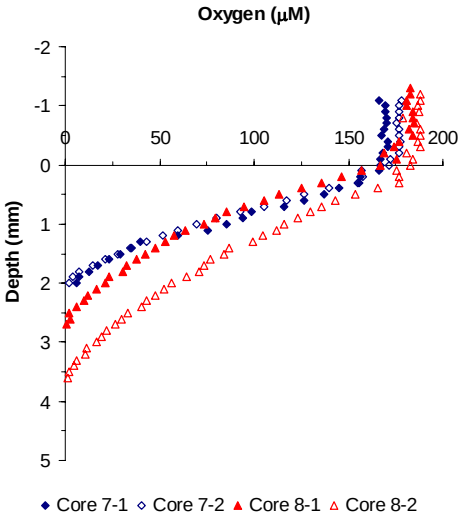

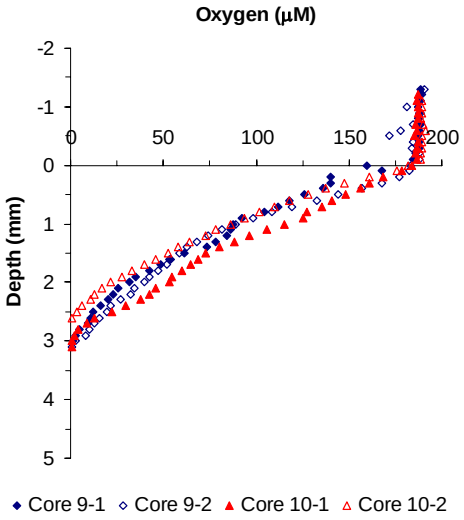

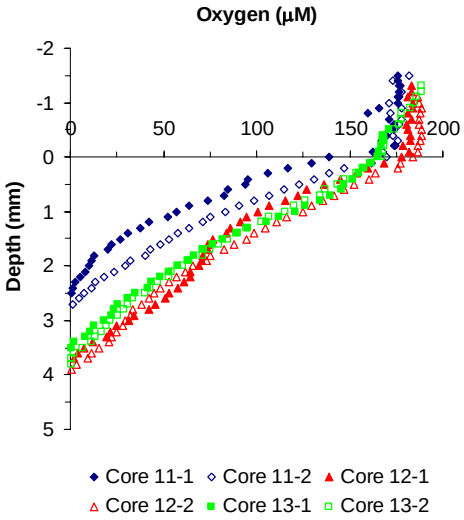

Low light (500 µmol photons m^{-2} s^{-1}) porewater O_2 profiles:

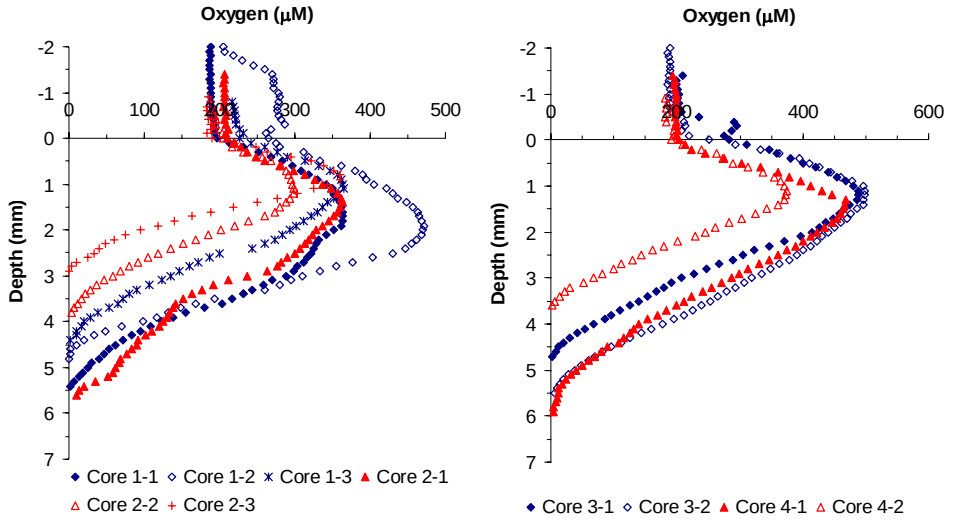

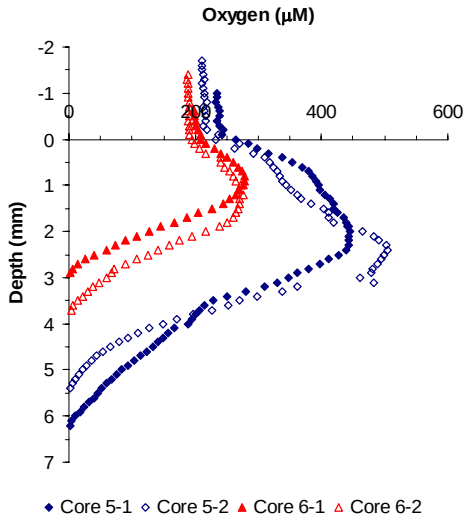

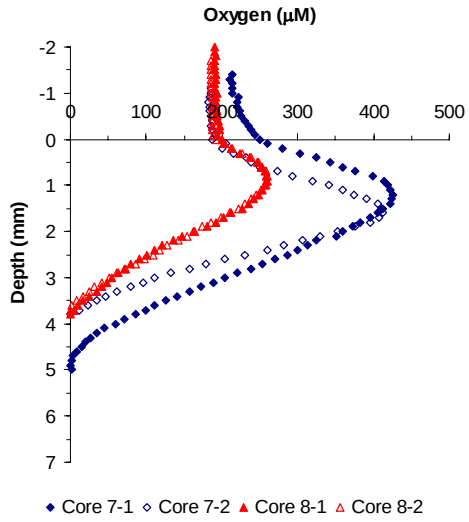

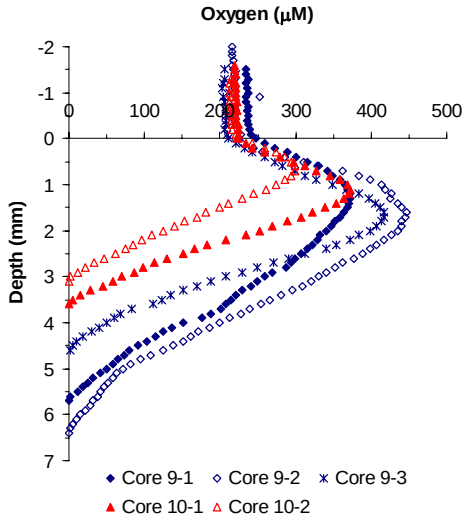

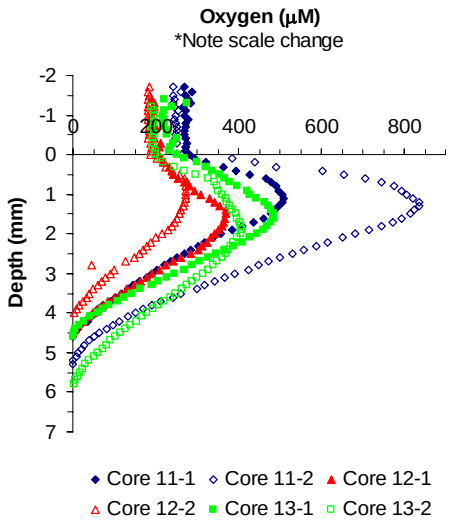

High light (1000 µmol photons m^{-2} s^{-1}) porewater O_2 profiles:

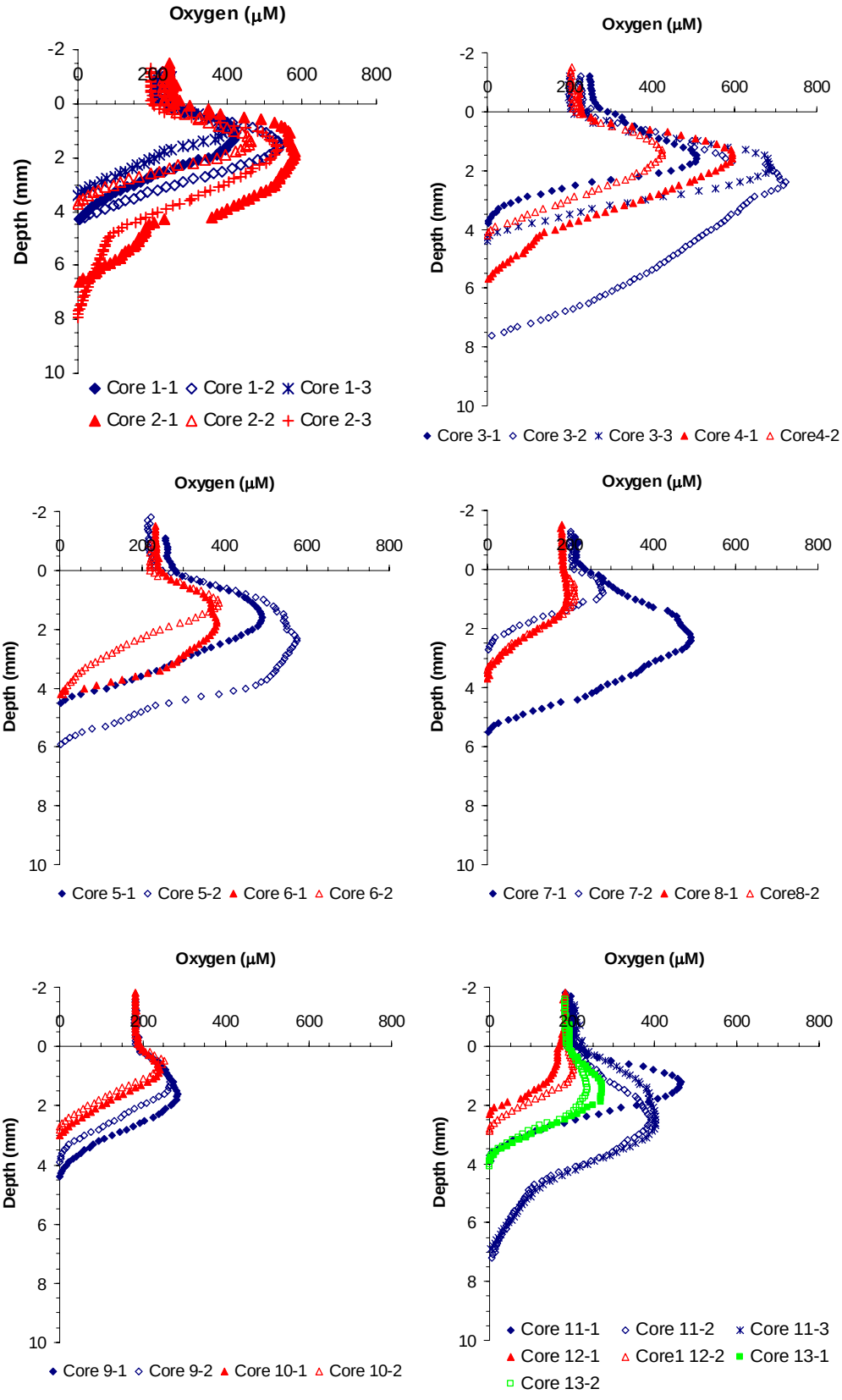

References

An S, and SB Joye (2001) Enhancement of coupled nitrification-denitrification by benthic photosynthesis in shallow estuarine sediments. *Limnology and Oceanography* 46:62-74.

Anderson IC, KJ McGlathery, and AC Tyler (2003) Microbial mediation of 'reactive' nitrogen transformations in a temperate lagoon. *Marine Ecology Progress Series* 246:73-84.

Armitage AR, TA Frankovich, KL Heck Jr., and JW Fourqurean (2005) Experimental nutrient enrichment causes complex changes in seagrass, microalgae, and macroalgae community structure in Florida Bay. *Estuaries* 28:422-434.

Baillie, PW 1986. Oxygenation and intertidal estuarine sediments by benthic microalgal photosynthesis. *Estuarine Coastal and Shelf Science* 22:143-159.

Berg P, N Risgaard-Petersen, and S Rysgaard (1998) Interpretation of measured concentration profiles in sediment porewater. *Limnology and Oceanography* 43:1500-1510.

—, S Rysgaard , P Funch , and MK Sejr (2001) Effects of bioturbation on solutes and solids in marine sediments. *Aquatic Microbial Ecology* 26:81-94.

Blicher-Mathiesen G, GW McCarty, and LP Nielsen (1998) Denitrification and degassing in groundwater estimated from dissolved dinitrogen and argon. *Journal of Hydrology* 208:16-24.

Boudreau BP (1997) Diagentic models and their implementation, Springer-Verlag, Berlin, Heidelberg, New York.

Boyer JN, JW Fourqurean, RD Jones (1999) Seasonal and long-term trends in the water quality of Florida Bay (1989-1997). *Estuaries* 22:417-430.

Cline JD (1969) Spectrophotometric determination of hydrogen sulfide in nautral waters. *Limnology and Oceanography* 14:454-458.

Cloern JE (1987) Turbidity as a control on phytoplankton biomass and productivity in estuaries. *Continental Shelf Research* 7:1367-1381.

Colijn F, and WN De Jonge (1984) Primary production of microphytobenthos in the Ems-Dollard estuary. *Marine Ecology Progress Series* 14:185-196.

Cornwell JC, WM Kemp, TM Kana (1999) Denitrification in coastal system: Methods, environmental controls and ecosystem level controls, a review. *Aquatic Ecology* 33:41-54.

Dalsgaard T (2003) Benthic primary production and nutrient cycling in sediments with benthic microalgae and transient accumulation of macroalgae. *Limnology and Oceanography* 48:2138-2150.

Davis MW, and CD McIntire (1983) Effect of physical gradients on the production dynamics of sediment-associated algae. *Marine Ecology Progress Series* 13:103-114.

Dong LF, CO Thornton, DB Nedwell, GJC Underwood (2000) Denitrification in sediments of the River Colne estuary, England. *Marine Ecology Progress Series* 203:109-122.

Eyre BD, and AJP Ferguson (2002) Comparison of carbon production and decomposition, benthic nutrient fluxes and denitrification in seagrass, phytoplankton, benthic microalgae- and macroalgae-dominated warm-temperate Australian lagoons. *Marine Ecology Progress Series* 229:43-59.

—, S Rysgaard, T Dalsgaard , and PB Christensen (2002) Comparison of isotope pairing and N-2: Ar methods for measuring sediment denitrification assumptions, modifications, and implications. *Estuaries* 25:1077-1087.

Ferguson AJP, BD Eyre, and JM Gay (2003) Organic matter and benthic metabolism in euphotic sediments along shallow sub-tropical estuaries, northern New South Wales, Australia. *Aquatic Microbial Ecology* 33:137-154.

Fourqurean JW, RD Jones, and JC Zieman (1993) Processes influencing water column nutrient characteristics and phosphorus limitation of phytoplankton biomass in Florida Bay, FL, USA: Inferences from spatial distributions. *Estuarine, Coastal and Shelf Science* 36:295-314.

— and MB Robblee (1999) Florida Bay: A history of recent ecological changes. *Estuaries* 22:345-357.

—, JC Zieman, and GVN Powell (1992) Phosphorus limitation of primary production in Florida Bay: Evidence from C-N-P ratios of the dominant Seagrass *Thalassia testudinum*. *Limnology and Oceanography* 37:162-171.

— and JC Zieman (2002) Nutrient content of the seagrass *Thalassia testudinum* reveals regional patterns of relative availability of nitrogen and phosphorus in Florida Keys USA. *Biogeochemistry* 61:229-245.

Gardner WS, MJ McCarthy, S An, D Sobolev, KS Sell, and D Brock (2005) Nitrogen fixation and dissimilatory nitrate reduction to ammonium (DNRA) support

nitrogen dynamics in Texas estuaries. *Limnology and Oceanography* 50:accepted.

Glud RN, M Kuhl, F Wenzhofer, and S Rysgaard (2002) Benthic diatoms of a high Arctic fjord (Young Sound, NE Greenland): importance for ecosystem primary production. *Marine Ecology Progress Series* 238:15-29.

—, JK Gundersen, NP Revsbech, and BB Jorgensen (1994) Effects on the benthic diffusive boundary layer imposed by microelectrodes. *Limnology and Oceanography* 39:462-467.

—, NB Ramsing, and NP Revsbech (1992) Photosynthesis and photosynthesis-coupled respiration in natural biofilms quantified with oxygen microsensors. *Journal of Phycology* 28:51-60.

Hall MO, MJ Durako, JW Fourqurean, and JC Zieman (1999) Decadal changes in seagrass distribution and abundance in Florida Bay. *Estuaries* 22:445-459.

Joint IR (1978). Microbial production of an estuarine mudflat. *Estuarine and Coastal Marine Science* 7:185-195.

Jorgensen BB, and NP Revsbech (1985) Diffusive boundary layers and the oxygen uptake of sediments and detritus. *Limnology and Oceanography* 30:111-122.

Joye SB, and JT Hollibaugh (1995) Influence of sulfide inhibition of nitrification on nitrogen regeneration in sediments. *Science* 270:623-625.

Kana TM, C Darkangelo, MD Hunt, JB Oldham, GE Bennett, and JC Cornwell (1994) Membrane inlet mass spectrometer for rapid high-precision determination of N_2, O_2 and Ar in environmental water samples. *Analytical Chemistry* 66:4166-4170.

—, Sullivan MB, Cornwell JC, Groszkowski KM (1998) Denitrification in estuarine sediments determined by membrane inlet mass spectrometry. *Limnology and Oceanography* 43:334-339.

—, and DL Weiss (2004) Comment on "Comparison of isotope pairing and N-2: Ar methods for measuring sediment denitrification" by B. D. Eyre, S. Rysgaard, T. Daisgaard, and P. Bondo Christensen. 2002. Estuaries 25: 1077-1087. *Estuaries* 27:173-176.

Kemp WM, JC Cornwell, MS Owens, L Pride, E Haberkern, and J Davis (2001) Role of benthic communities in the cycling and balance of nitrogen in Florida Bay. U.S. Environmental Protection Agency Final Report.

Krenn J (2003) The influence of microphytobenthos on resuspension in shallow estuaries: a comparison between the Florida and Chesapeake Bays. University of Maryland Research Experience for Undergraduates (REU) Final Report.

Krom MD (1991) Importance of benthic productivity in controlling the flux of dissolved inorganic nitrogen through the sediment-water interface in a hypertrophic marine ecosystem. *Marine Ecology-Progress Series* 78:163-172.

Kuhl M, RN Glud, H Ploug, and NB Ramsing (1996) Microenvironmental control of photosynthesis and photosynthesis-coupled respiration in an epilithic cyanobacterial biofilm. *Journal Of Phycology* 32:799-812.

Lavery PS, CE Oldham, and M Ghisalberti (2001) The use of Fick's First Law for predicting porewater nutrient fluxes under diffusive conditions. *Hydrological Processes* 15:2435-2451.

Leach, JH (1970) Epibenthic algal production in an intertidal mudflat. *Limnology and Oceanograhpy*15:514-521.

Lee K-S, and KH Dunton (2000) Diurnal changes in pore water sulfide concentrations in the seagrass *Thalassia testudinum* beds: the effects of seagrasses on sulfide dynamics. *Journal of Experimental Marine Biology and Ecology* 255:201-214.

:MacIntyre HL, and JJ Cullen (1996) Primary production by suspended and benthic microalgae in a turbid estuary: Time-scales of variability in San Antonio Bay, Texas. *Marine Ecology Progress Series* 145: 245-368.

—, RJ Geider, and DC Miller (1996) Microphytobenthos: The ecological role of the "secret garden" of unvegetated, shallow-water marine habitats. 1. Distribution, abundance and primary production. *Estuaries* 19:186-201.

Marshall N, CA Oviatt, and DM Skauen (1971) Productivity of the benthic microflora of shoal estuarine environments in southern New England. *International Revue der gesamten Hydrobiologie* 56: 947-956.

—, DM Skauen, HC Lampe and CA Oviatt (1972) A guide to the measurement of marine production under some special conditions. P. 37-44. Monographs on Oceanographic Methodology, 3 ,UNESCO. Paris.

Matheke GEM and R. Horner (1974) Primary productivity of the benthic microalgae in the Chukchi Sea near Barow, Alaska. *Journal of the Fisheries Research Board of Canada* 31:1779-1786,

McCarthy MJ, and WS Gardner (2003) An application of membrane inlet mass spectrometry to measure denitrification in a recirculating mariculture system. *Aquaculture* 218:341-355.

McGlathery KJ, IC Anderson, and AC Tyler (2001) Magnitude and variability of benthic and pelagic metabolism in a temperate coastal lagoon. *Marine Ecology Progress Series* 216:1-15.

Middelburg JJ, C Barranguet, HTS Boschker, PMJ Herman, T Moens, and CHR Heip (2000) The fate of intertidal microphytobenthos carbon: An in situ C-13-labeling study. *Limnology and Oceanography* 45:1224-1234.

Mitbavkar S, and AC Anil (2004) Vertical migratory rhythms of benthic diatoms in a tropical intertidal sand flat: influence of irradiance and tides. *Marine Biology* 145:9-20.

Nagel ED (2004) Nitrogen fixation in benthic microalgal mats: An important, internal source of "new" nitrogen to the benthic communities of Florida Bay. Masters Thesis. University of Maryland, College Park..

Nelson DC, NP Revsbech, and BB Jorgensen (1986) Microoxic-anoxic niche of *Beggiatoa spp* - microelectrode survey of marine and freshwater strains. *Applied And Environmental Microbiology* 52:161-168.

Nuttle WK, JW Fourqurean, BJ Cosby, JC Zieman,and MB Robblee (2000) Influence of net freshwater supply on salinity in Florida Bay. *Water Resources Research* 36:1805-1822.

Parsons TR, Y Maita, and CM Lalli (1984) A Manual of Chemical and Biological Methods for Seawater Analysis. Pergamon Press, Oxford, New York.

Pinckney J, and RG Zingmark (1991) Effects Of Tidal Stage And Sun Angles On Intertidal Benthic Microalgal Productivity. *Marine Ecology-Progress Series* 76:81-89.

— and — (1993) Biomass and Production of Benthic Microalgal Communities in Estuarine Habitats. *Estuaries* 16:887-897.

Plante-Cuny MR, and A Bodoy (1987) Biomasse et production primaire du phytoplankton et du microphytobenthos de duex biotopes sableux (Golfe de Fos, France) *Oceanology Acta* 10:223-237.

Poe AC, MF Pichler, SP Thompson, and HW Paerl (2003) Denitrification in a constructed wetland receiving agricultural runoff. *Wetlands* 23:817-826.

Revsbech NP, and BB Jorgensen (1983) Photosynthesis Of Benthic Microflora Measured With High Spatial-Resolution By The Oxygen Microprofile Method - Capabilities And Limitations Of The Method. *Limnology and Oceanography* 28:749-756.

—, BB Jorgensen, TH Blackburn, and Y Cohen (1983) Microelectrode studies of Tthe photosynthesis snd O_2, H_2S, and pH profiles of a microbial mat. *Limnology and Oceanography* 28:1062-1074.

—, BB Jorgensen, and O Brix (1981) Primary production of microalgae in sediments measured by oxygen microprofile, $H^{14}CO_3$-fixation, and oxygen exchange methods. *Limnology and Oceanography* 26:717-730.

Risgaard-Petersen N, S Rysgaard, LP Nielsen, and NP Revsbech (1994) Diurnal variation of denitrification and nitrification in sediments colonized by benthic microphytes. *Limnology and Oceanography*39:573-579.

Riznyk RZ, JI Edens and RC Libby (1978) Production of epibenthic diatoms in a outhern Califronia impounded estuary. *Journal of Phycology* 14:273-279.

Rizzo WM, and RL Wetzel (1985) Intertidal and shoal benthic community metabolism in a temperate estuary: Studies of spatial and temporal scales of variability. *Estuaries* 8: 342-351.

Robblee MB, TR Barber, PR Carlson, MJ Durako, JW Fourqurean , LK Muehlstein, D Porter, LA Yarbro, RT Zieman, and JC Zieman (1991) Mass mortality of the tropical seagrass *Thalassia testudinum* in Florida Bay (USA). *Marine Ecology-Progress Series* 71:297-299.

Rysgaard S, PB Christensen, and LP Nielsen (1995) Seasonal variation in nitrification and denitrification in estuarine sediment colonized by benthic microalgae and bioturbating infauna. *Marine Ecology-Progress Series* 126:111-121.

—, PB Christensen, MV Sorensen, P Funch, and P Berg (2000) Marine meiofauna, carbon and nitrogen mineralization in sandy and soft sediments of Disko Bay, West Greenland. *Aquatic Microbial Ecology* 21:59-71.

—, N Risgaard-Petersen, and NP Sloth (1996) Nitrification, denitrification, and nitrate ammonification in sediments of two coastal lagoons in Southern France. *Hydrobiologia* 329:133-141.

Sand-Jensen K, and SL Nielsen (2004) Estuarine primary producers. In: Nielsen SL, Banta GT, Pedersen MF (eds) Estuarine nutrient cycling: the influence of primary producers, Vol 2. Kluwer Academic Publishers, Dordrecht, Boston, London, p 17-57.

Shaffer GP, and CP Onuf (1983) An analysis of factors influencing the primary production of the benthic microflora in a southenr California. *Netherlands Journal of Sea Research* 17: 126-144.

Sullivan M, and C Moncreiff (1988) Primary production of edaphic algal communities in a Mississippi salt marsh. *Journal of Phycology*24:49-58.

Sundback K, B Jonsson, P Nilsson, and I Lindstrom (1990) Impact of accumulating drifting macroalgae on a shallow water sediment system - an experimental study. *Marine Ecology Progress Series* 58:261-274.

—, F Linares, F Larson, A Wulff, and A Engelsen (2004) Benthic nitrogen fluxes along a depth gradient in a microtidal fjord: The role of denitrification and microphytobenthos. *Limnology and Oceanography* 49:1095-1107.

—, and A Miles (2000) Balance between denitrification and microalgal incorporation of nitrogen in microtidal sediments, NE Kattegat. *Aquatic Microbial Ecology* 22:291-300.

—, A Miles, and E Goransson (2000) Nitrogen fluxes, denitrification and the role of microphytobenthos in microtidal shallow-water sediments: an annual study. *Marine Ecology Progress Series* 200:59-76.

—, A Miles, S Hulth, L Pihl, P Engstrom, E Selander,and A Svenson (2003) Importance of benthic nutrient regeneration during initiation of macroalgal blooms in shallow bays. *Marine Ecology Progress Series* 246:115-126.

Thornton DCO, LF Dong, GJC Underwood, and DB Nedwell (2002) Factors affecting microphytobenthic biomass, species composition and production in the Colne Estuary (UK). *Aquatic Microbial Ecology* 27:285-300.

Tiedje JM, S Simkins, and PM Groffman (1989) Perspectives on measurement of denitrification in the field including recommended protocols for acetylene based methods. *Plant And Soil* 115:261-284.

Van Heukelem L, AJ Lewitus, TM Kana, and NE Craft (1994) Improved separations of phytoplankton pigments using temperature-controlled high performance liquid chromatography. *Marine Ecolgoy Progress Series* 114:303-313.

VanRaalte CD, I Valiela, and JM Teal (1976) Production of benthic salt marsh algae: Light and nutrient limitation. *Limnology and Oceanography* 21: 862-872.

Varela M, and E Penas (1985) Primary production of benthic microalgae in an intertidal sand flat of the Ria de Arosa, NW Spain. *Marine Ecology Progress Series* 25: 111-119.

Wetzel RG, and GE Likens (2000) Limnological analyses, Springer-Verlag, New York, Berlin, Heidelberg

Zieman JC, JW Fourqurean, and RL Iverson (1989) Distribution, Abundance And Productivity Of Seagrasses And Macroalgae In Florida Bay. *Bull Mar Sci* 44:292-311.